Examining the Association between Posttraumatic Stress Disorder and Disruptions in Cortical Networks Identified Using Data-Driven Methods

Jin Yang[1], Ashley A. Huggins[2,3], Delin Sun[2,3,4], C. Lexi Baird[2,3], Courtney C. Haswell[2,3], Jessie L. Frijling[5], Miranda Olff[5,6], Mirjam van Zuiden[5], Saskia B.J. Koch[5,7], Laura Nawijn[5], Dick J. Veltman[5], Benjamin Suarez-Jimenez[8], Xi Zhu[9,10], Yuval Neria[9,10], Anna R. Hudson[11], Sven C. Mueller[11], Justin T. Baker[12,13], Lauren A.M. Lebois[12,14], Milissa L. Kaufman[12,15], Rongfeng Qi[16], Guang Ming Lu[16], Pavel Říha[17,18], Ivan Rektor[18], Emily L. Dennis[19,20], Christopher R.K. Ching[21], Sophia I. Thomopoulos[21], Lauren E. Salminen[21], Neda Jahanshad[21], Paul M. Thompson[21], Dan J. Stein[22], Sheri M. Koopowitz[22], Jonathan C. Ipser[22], Soraya Seedat[23], Stefan du Plessis[23], Leigh L. van den Heuvel[23], Li Wang[24,25], Ye Zhu[24,25], Gen Li[24,25], Anika Sierk[26], Antje Manthey[26], Henrik Walter[26], Judith K. Daniels[27], Christian Schmahl[28], Julia I. Herzog[28], Israel Liberzon[29], Anthony King[30], Mike Angstadt[30], Nicholas D. Davenport[31,32], Scott R. Sponheim[31,32], Seth G. Disner[31,32], Thomas Straube[33], David Hofmann[33], Daniel W. Grupe[34], Jack B. Nitschke[35], Richard J. Davidson[34,35,36], Christine L. Larson[37], Terri A. deRoon-Cassini[38,39], Jennifer U. Blackford[40,41], Bunmi O. Olatunji[42], Evan M. Gordon[1], Geoffrey May[43,44,45,46], Steven M. Nelson[43,44,45,46], Chadi G. Abdallah[47,48], Ifat Levy[49,50,51,52,53], Ilan Harpaz-Rotem[47,51,53], John H. Krystal[47,53], Rajendra A. Morey[2,3], Aristeidis Sotiras[1,54]

Corresponding Author:
Rajendra Morey MD
Duke Brain Imaging and Analysis Center
Duke University School of Medicine
40 Medicine Circle Drive
Durham, NC 27710
Email: rajendra.morey@duke.edu

Keywords:
Posttraumatic Stress Disorder (PTSD), Cortical thickness, Psychological trauma, Non-negative matrix factorization (NMF)

Affiliations:
1. Department of Radiology, Washington University in St. Louis, St. Louis, MO, USA
2. Duke-UNC Brain Imaging and Analysis Center, Duke University, Durham, NC, USA
3. Mid-Atlantic Mental Illness Research Education and Clinical Center, Durham VA Medical Center, Durham, NC, USA

4. Department of Psychology, The Education University of Hong Kong, Hong Kong, China
5. Department of Psychiatry, Amsterdam University Medical Center, Amsterdam, the Netherlands
6. ARQ National Psychotrauma Centre, Diemen, the Netherlands.
7. Donders Institute for Brain, Cognition and Behavior, Centre for Cognitive Neuroimaging, Radboud University Nijmegen, Nijmegen, the Netherlands
8. Del Monte Institute for Neuroscience, University of Rochester Medical Center, Rochester, NY, USA
9. Department of Psychiatry, Columbia University Medical Center, New York, NY, USA.
10. New York State Psychiatric Institute, New York, NY, USA.
11. Department of Experimental Clinical and Health Psychology, Ghent University, Ghent, Belgium
12. Department of Psychiatry, Harvard Medical School, Boston, MA, USA
13. Institute for Technology in Psychiatry, McLean Hospital, Harvard University, Belmont, MA, USA
14. Division of Depression and Anxiety Disorders, McLean Hospital, Belmont, MA, USA
15. Division of Women's Mental Health, McLean Hospital, Belmont, MA, USA
16. Department of Medical Imaging, Jinling Hospital, Medical School of Nanjing University, Jiangsu, China
17. First Department of Neurology, St. Anne's University Hospital and Faculty of Medicine, Masaryk University, Brno, Czech Republic
18. CEITEC-Central European Institute of Technology, Multimodal and Functional Neuroimaging Research Group, Masaryk University, Brno, Czech Republic
19. Department of Neurology, University of Utah, Salt Lake City, UT, USA
20. George E. Wahlen Veterans Affairs Medical Center, Salt Lake City, UT, USA
21. Imaging Genetics Center, Mark & Mary Stevens Neuroimaging & Informatics Institute, Keck School of Medicine of USC, Marina del Rey, CA, USA
22. Department of Psychiatry and Neuroscience Institute, University of Cape Town, Cape Town, South Africa
23. Department of Psychiatry, Stellenbosch University, Cape Town, South Africa
24. Laboratory for Traumatic Stress Studies, Chinese Academy of Sciences Key Laboratory of Mental Health, Institute of Psychology, Chinese Academy of Sciences, Beijing, China
25. Department of Psychology, University of Chinese Academy of Sciences, Beijing, China
26. University Medical Centre Charité, Berlin, Germany
27. Department of Clinical Psychology, University of Groningen, Groningen, the Netherlands
28. Department of Psychosomatic Medicine and Psychotherapy, Central Institute of Mental Health, Medical Faculty Mannheim, Heidelberg University, Heidelberg, Germany
29. Department of Psychiatry and Behavioral Science, Texas A&M University, College Station, TX, USA
30. Department of Psychiatry, University of Michigan, Ann Arbor, MI, USA
31. Minneapolis VA Health Care System, Minneapolis, MN, USA
32. Department of Psychiatry, University of Minnesota, Minneapolis, MN, USA
33. Institute of Medical Psychology and Systems Neuroscience, University of Münster, Münster, Germany

34. Center for Healthy Minds, University of Wisconsin-Madison, Madison, WI, USA
35. Department of Psychiatry, University of Wisconsin-Madison, Madison, WI, USA
36. Department of Psychology, University of Wisconsin-Madison, Madison, WI, USA
37. Department of Psychology, University of Wisconsin-Milwaukee, Milwaukee, WI, USA
38. Division of Trauma and Acute Care Surgery, Department of Surgery, Medical College of Wisconsin, Milwaukee, WI, USA
39. Comprehensive Injury Center, Medical College of Wisconsin, Milwaukee, WI, USA
40. Munroe-Meyer Institute, University of Nebraska Medical Center, Omaha, NE, USA
41. Department of Psychiatry and Behavioral Sciences, Vanderbilt University Medical Center, Nashville, TN, USA
42. Department of Psychology, Vanderbilt University, Nashville, TN, USA
43. Veterans Integrated Service Network-17 Center of Excellence for Research on Returning War Veterans, Waco, TX, USA
44. Department of Psychology and Neuroscience, Baylor University, Waco, TX, USA
45. Center for Vital Longevity, School of Behavioral and Brain Sciences, University of Texas at Dallas, Dallas, TX, USA
46. Department of Psychiatry and Behavioral Science, Texas A&M University Health Science Center, Bryan, TX, USA
47. Department of Psychiatry, Yale University School of Medicine, New Haven, CT, USA
48. Department of Psychiatry of Behavioral Sciences, Baylor College of Medicine, Houston, TX, USA
49. Department of Comparative Medicine, Yale University, New Haven, CT, USA
50. Department of Neuroscience, Yale University, New Haven, CT, USA
51. Department of Psychology, Yale University, New Haven, CT, USA
52. Wu Tsai Institute, Yale University, New Haven, CT, USA
53. Division of Clinical Neuroscience, National Center for PTSD, West Haven, CT, USA
54. Institute for Informatics, Washington University in St. Louis, St. Louis, MO, USA

0. Abstract

Posttraumatic stress disorder (PTSD) is associated with lower cortical thickness (CT) in prefrontal, cingulate, and insular cortices in diverse trauma-affected samples. However, some studies have failed to detect differences between PTSD patients and healthy controls or reported that PTSD is associated with greater CT. Using data-driven dimensionality reduction, we sought to conduct a well-powered study to identify vulnerable networks without regard to neuroanatomic boundaries. Moreover, this approach enabled us to avoid the excessive burden of multiple comparison correction that plagues vertex-wise methods. We derived structural covariance networks (SCNs) by applying non-negative matrix factorization (NMF) to CT data from 961 PTSD patients and 1,124 trauma-exposed controls without PTSD. We used regression analyses to investigate associations between CT within SCNs and PTSD diagnosis (with and without accounting for the potential confounding effect of trauma type) and symptom severity in the full sample. We performed additional regression analyses in subsets of the data to examine associations between SCNs and comorbid depression, childhood trauma severity, and alcohol abuse. NMF identified 20 unbiased SCNs, which aligned closely with functionally defined brain networks. PTSD diagnosis was most strongly associated with diminished CT in SCNs that encompassed the bilateral superior frontal cortex, motor cortex, insular cortex, orbitofrontal cortex, medial occipital cortex, anterior cingulate cortex, and posterior cingulate cortex. CT in these networks was significantly negatively correlated with PTSD symptom severity. Collectively, these findings suggest that PTSD diagnosis is associated with widespread reductions in CT, particularly within prefrontal regulatory regions and broader emotion and sensory processing cortical regions.

1. Introduction

Posttraumatic stress disorder (PTSD) is a debilitating psychiatric illness with a lifetime prevalence of nearly 10% [1]. PTSD is characterized by a constellation of symptoms including intrusive memories, avoidance, negative alterations in cognition and mood, and hyperarousal [2]. Consistent with this phenotype, a wealth of research has demonstrated that PTSD is associated with several structural and functional differences in brain regions involved in affect, cognition, and memory [3–5].

As a metric of grey matter integrity, cortical thickness studies have been particularly illuminating for understanding the pathophysiology of PTSD. In general, PTSD has been associated with lower cortical thickness in regions including the prefrontal [6–11], cingulate [6,12–14], and insular [15] cortices in diverse trauma-affected samples, including veterans [6,7,9–11,15–17], and individuals with a history of childhood trauma [6,8,14]. Notably, some studies have also shown that greater cortical thickness may be an important marker of resilience and recovery in trauma-exposed samples [18–21].

However, some studies have failed to detect differences between PTSD patients and healthy controls [22–29], or have suggested that PTSD is associated with greater cortical thickness in specific regions, including the precuneus [30], calcarine cortex [31], and superior and frontal gyri [21,32]. PTSD is highly heterogeneous – both in symptom profiles [33] and trauma type – researchers have proposed that differences in cortical thickness may be related to specific populations and/or symptom clusters [13,26]. However, most efforts to characterize cortical thickness differences implicated in PTSD have also relied upon small samples and region of interest (ROI) approaches [25,28,29] or trauma naïve [24,26,27] individuals. Indeed, results from recent meta-analytic work suggest different cortical thickness correlates emerge depending on whether the control group was trauma-exposed or not [32]. Although focusing on specific regions of the brain involved with neurobiological systems implicated in PTSD symptoms has proven to be an effective strategy, regional differences in cortical thickness may

not necessarily adhere to strict neuroanatomical boundaries or may be associated with brain regions not previously implicated in PTSD.

To this end, novel, data-driven methods, such as non-negative matrix factorization (NMF), may provide powerful insights about the localized effects of PTSD on cortical thickness. NMF is an unsupervised machine learning method for multivariate analysis of high-dimensional neuroimaging data. NMF factorizes data under non-negativity constraints leading to a parts-based representation, which enhances interpretability and statistical power [34,35]. Applied to anatomical data, NMF can elucidate patterns in cortical thickness variation that are shared within a sample, which may not adhere to neuroanatomical boundaries [35]. NMF-derived structural covariance networks map onto functionally-derived brain networks [35,36], and can aid in the interpretability of cortical thickness findings related to disease states and behavioral phenotypes [37]. Although no published studies have used NMF to examine structural measures in PTSD, the technique has been successfully implemented in various samples to identify cortical thickness differences related to neurodevelopment [35,38,39], impulsivity [40], and other psychopathology [41–44].

Leveraging a large, multisite dataset from the PGC-ENIGMA PTSD Working Group, we employed NMF to identify structural covariance networks (SCNs) and examine differences in cortical thickness within these networks associated with PTSD. In a series of linear regression models, we tested whether PTSD diagnosis and severity were associated with abnormalities within NMF-derived networks. Additionally, we examined the potential confounding effect of trauma type on PTSD-associated group differences by including it as a binary categorical covariate. Lastly, to examine the specificity of effects, we also ran models that examined associations between SCNs and major depressive disorder (MDD), alcohol abuse and childhood trauma severity, respectively. These disorders are known to have a high co-occurrence with PTSD and have also been linked to cortical thickness alterations [8,37,45–49]. We conducted these additional analyses on subsets of the data where necessary information was available. While we hypothesized that PTSD would be associated with lower cortical thickness in specific

structural networks in prefrontal [6–11] and cingulate [6,12–14] cortices, the data-driven capability of NMF enabled us to identify heretofore undocumented areal features on the cortical surface associated with PTSD.

2. Methods

2.0 Overview

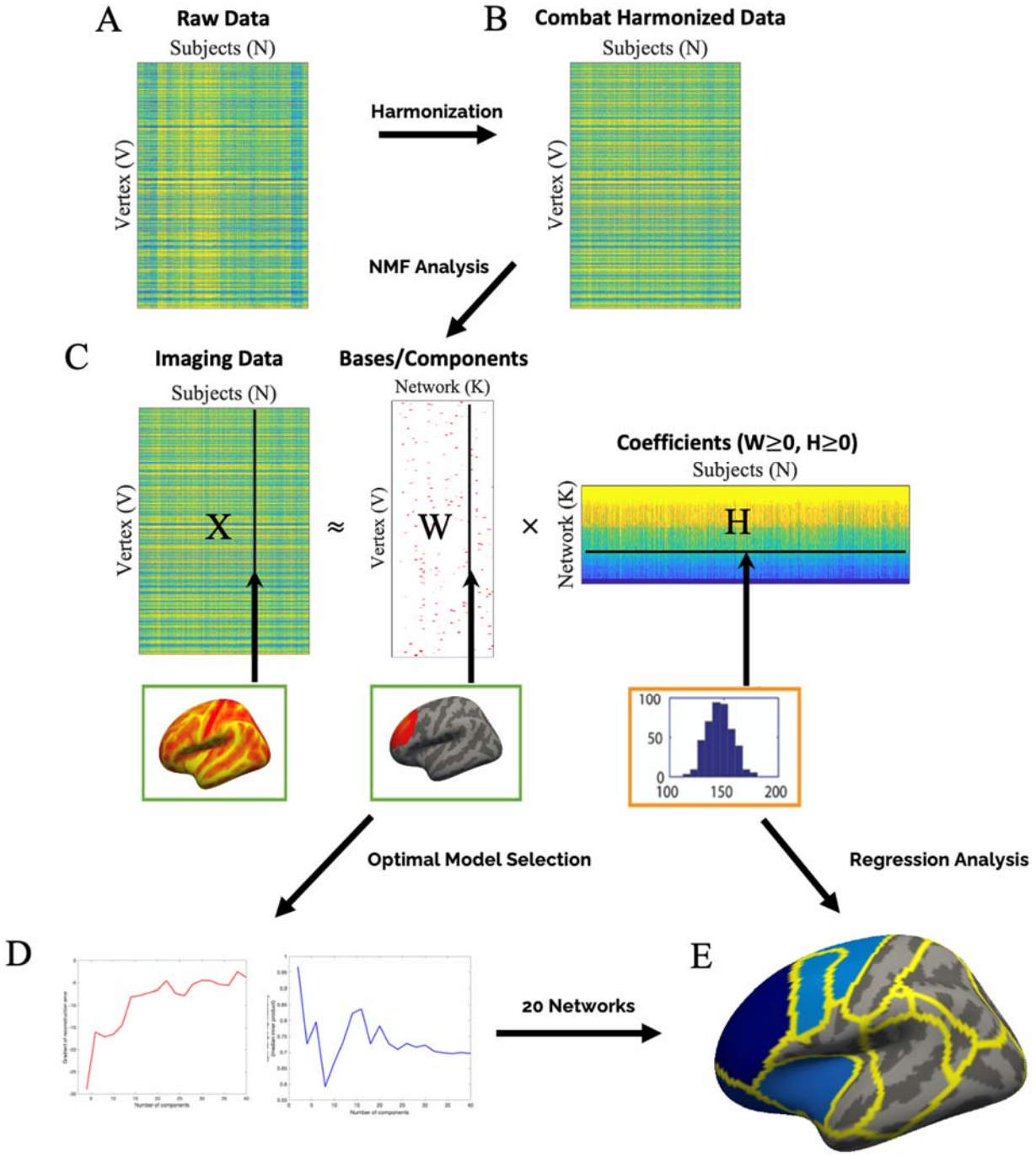

Data analysis consisted of 8 major steps (**Fig. 1**). (1) We assembled imaging, clinical, and demographic data from 22 sites participating in ENIGMA-PTSD and harmonized clinical variables, including PTSD and symptom severity scores. (2) We created vertex-wise cortical surface maps for each participant using the FreeSurfer software suite [50] (**Fig. 1A**). (3) We performed harmonization of cortical thickness data to account for site and scanner effects using *ComBat* [51] (**Fig. 1B**). (4) We applied a multivariate, hypothesis-free method, non-negative matrix factorization (NMF), to identify SCNs (**Fig. 1C**). (5) Split-half reproducibility analysis and reconstruction error evaluation were used to select the optimal number of components (**Fig. 1D**). (6) We then conducted regression analyses to investigate respective associations between cortical thickness and PTSD diagnosis and symptom severity. The mean cortical thickness of 20 covariance networks from step #4 were used as the dependent variables in regression analyses. Regressors were added to the model to test for potential confounding effects of demographic variables, including sex, age, and the quadratic effect of age (**Fig. 1E**). (7) We conducted a confirmatory analysis with more homologous case-control samples without age or sex differences. (8) We conducted regression analyses to investigate the respective associations between comorbid depression, childhood trauma severity, and comorbid alcohol abuse and cortical thickness within SCNs.

2.1 Participants

Population information and T1-weighted magnetic resonance imaging (MRI) data were collected from 2,085 individuals who were assigned to the PTSD group (n=961) or trauma-exposed non-PTSD control group (n=1,124). Participant data was shared by 22 sites from seven countries on four continents. Descriptive information on the samples is provided in **Table S1**. Inclusion and exclusion criteria for each site are summarized in **Table S2**. For all sites (and sub-sites) where imaging data and demographic data were collected, current PTSD was diagnosed according to Diagnostic and Statistical Manual of Mental Disorders (DSM) IV or 5 criteria, using the following standard instruments: Clinician-Administered PTSD Scale-IV (CAPS-4; 10 sites, 14 sub-sites; DSM-IV), CAPS-5 (5 sites, 8 subsites; DSM-5), Structured Clinical Interview (SCID-4; 4

sites; DSM-IV), Mini International Neuropsychiatric Interview 6.0.0 (2 sites, DSM-IV), PTSD Checklist-5 (PCL-5; 2 sites; DSM-5), and PTSD Checklist-Civilian Version (PCL-C; 1 site, DSM- IV). All study sites obtained approval from local institutional review boards or ethics committees. All participants provided written informed consent.

2.2 Imaging acquisition and processing

High-resolution 3D T1-weighted brain structural MRI (sMRI) scans were collected at contributing laboratories. Anatomical brain images were preprocessed at Duke University through a standardized neuroimaging and quality control pipeline developed by the ENIGMA Consortium (http://enigma.ini.usc.edu/protocols/imaging-protocols/) [52]. The raw T1 sMRI data were pre-processed using the *FreeSurfer* software suite [50] (version 5.3.0, 6.0.0 or 7.1.0; see Table S1) to create cortical thickness maps for each individual subject, which were mapped to the fsaverage5 template space. Following our previous works [35,37,44], cortical thickness maps were smoothed using an isotropic Gaussian filter kernel with full width at half maximum (FWHM) size of 20 mm (**Fig. 1A**; Sec. S1.1).

2.3 Harmonization

An important challenge when analyzing consortium data is variation introduced by site-specific acquisition protocols and MRI scanners, which may interact with site-specific demographic and clinical profiles. To address this challenge, we employed harmonization using ComBat [51,53,54] (**Fig. 1B**). ComBat removes undesired site-associated differences while preserving inherent biological variance in the data [51]. In the present study, three variables (i.e., age, sex, and PTSD diagnosis) were included as covariates to preserve associated biological variability. Batches were created to remove unwanted variability associated with sites and scanners. The ComBat approach was implemented using scripts (https://github.com/Jfortin1/ComBatHarmonization) running on MATLAB, version R2018b.9.5.0.1033004.

2.4 Non-negative matrix factorization analysis

We used non-negative matrix factorization (NMF) to identify structural networks where cortical thickness covaries consistently across participants (**Fig. 1C**). NMF is an unsupervised, data-driven technique that factors the data by positively weighting cortical elements that covary. NMF yields a parts-based representation, which is more interpretable and reproducible than representations obtained by other decomposition techniques (e.g., Principal Component Analysis and Independent Component Analysis) [34,35] and has greater statistical power than standard mass univariate analyses [40,41]. Details regarding the formalization of NMF have been provided elsewhere [34,35] and in the Supplementary Material (see Sec. S1.2).

The NMF algorithm may approximate the input data at different resolutions depending on the user-specified parameter K that denotes the number of networks. Accordingly, we systematically examined multiple NMF resolutions ranging from 2 to 40 networks (in steps of 2). To determine the optimal number of components, we performed a split-half reproducibility analysis and evaluated the reconstruction quality (see **Fig. 1D** and Sec. S1.2). The goal was to select a model that was reproducible and fit the data well.

2.5 Statistical analyses

First, we examined associations between categorical PTSD diagnosis and brain structure (**Fig. 1E**). We used quadratic regression analysis to evaluate cortical thickness differences in each network between PTSD and control groups, after controlling for sex, age, and quadratic effects of age. Specifically, the following group-comparison model was employed, with CT_{SCN} representing the average cortical thickness in an NMF-derived SCN:

$$CT_{SCN} \sim age + age^2 + sex + PTSD \quad \text{(Eq. 1)}$$

The trauma type was also added to the statistical model as a binary categorical covariate (military vs. civilian) for all sites and cohorts (Table S1) to examine its potential confounding effect on PTSD-associated group differences. Interactions of age by diagnosis and sex by diagnosis terms were then added to the statistical model to examine potential interactive effects of these factors on group differences.

Second, associations between cortical thickness and dimensional posttraumatic stress symptom (PTSS) severity were examined. Instruments for assessing PTSS severity varied by site. Score homogenization was accomplished by calculating the percentage of the severity score relative to the maximum score possible for each instrument (Table S3). Most (20 out of 22, Table S3) sites assessed PTSS severities in trauma-exposed control subjects, resulting in a sub-sample of 1,995 subjects (from both PTSD and control groups) with normalized PTSS severity scores. We used quadratic regression analysis to examine associations between cortical thickness in each network and PTSS severity, with adjustments for sex, age, and quadratic effects of age:

$$CT_{SCN} \sim age + \ age^2 + sex + PTSS\ severity \text{ (Eq. 2)}$$

Lastly, we examined the respective associations of comorbid depression, childhood trauma severity, and comorbid alcohol abuse (referred to as 'confounder' in Eq. 3) with cortical thickness alternations. Specifically, we used regression analyses to examine whether cortical thickness within each network was associated with each of these confounders, after accounting for sex, age, and quadratic effects of age:

$$CT_{SCN} \sim age + \ age^2 + sex + confounder \text{ (Eq. 3)}$$

This analysis was performed only for the subsets of the data that included the necessary information. In these subsets of the data, we performed two additional regression analyses. First, we included categorical PTSD diagnosis in the regression model to examine potential

confounding effects of comorbid depression, childhood trauma severity, and comorbid alcohol abuse (referred to as 'confounder' in Eq. 4) on PTSD-associated group differences:

$$CT_{SCN} \sim age + age^2 + sex + PTSD + confounder \text{ (Eq. 4)}$$

Second, we examined associations between categorical PTSD diagnosis and brain structure when not controlling for the confounder (Eq. 1).

Comorbid depression was modeled as a binary index distinguishing high (N = 316) vs. low (N = 1,565) depression symptom severity based on either questionnaire-specific depression cut-off scores or SCID diagnosis (Table S3). We use the shorthand designation of *depression* throughout to refer to severity of depressive symptoms as reflected by the derived binary label. Thus, in the present context, *depression* does not necessarily meet strict diagnostic criteria for major depressive disorder per the DSM. The derived binary categorical variable was included as covariate in the regression analysis (Eq. 3) to investigate the association between the cortical thickness within each SCN and depression. This analysis was performed separately for PTSD patients only (N=863) and the full sub-sample (N=1,881). Lastly, two separate regression analyses (Eqs. 1 and 4) were performed in the full sub-sample (N=1,881) to examine group differences associated with PTSD and to assess the potential confounding effect of depression.

Childhood trauma severity was evaluated by the total Childhood Trauma Questionnaire (CTQ) [55] for each subject and was recorded as the total CTQ value for each site (Table S3; Fig. S1). The total CTQ value was transformed to remove skewness (see Sec. S1.3) and was then included as covariate in the regression model (Eq. 3) to examine the associations between the cortical thickness within each SCN and childhood trauma severity. This analysis was conducted on the full sub-sample (N=589), as well as separately on PTSD patients (N=355) and control subjects (N=234). Lastly, two separate regression analyses (Eqs. 1 and 4) were performed in the full sub-sample (N=589). These analyses examined group differences associated with PTSD and assessed the potential confounding effect of childhood trauma severity.

Comorbid alcohol abuse was assessed through the diagnosis of alcohol abuse disorder (AUD) by different AUD tools (Table S3). Based on exclusion criteria and diagnostic information, we defined a binary index to distinguish potential alcohol abuse disorder (N=110) vs. non-comorbid alcohol (N=963) (Table S4). The binary label was then included as covariate in the regression model (Eq. 3) to examine the associations between the cortical thickness within each SCN and alcohol abuse. Separate analyses were performed for PTSD patients (N=469) and the full sub-sample (N=1,073). Lastly, two separate regression analyses (Eqs. 1 and 4) were performed in the full sub-sample (N=1,073). These analyses examined group differences associated with PTSD and assessed the potential confounding effect of alcohol abuse.

To account for multiple comparisons across all estimations, we controlled the false discovery rate (FDR) [56] as implemented in R [57]. An FDR corrected $p < 0.05$ was considered significant. All statistical analyses were performed using R, version 3.5.1.

3. Results

3.1 Sample characteristics

Table 1. Demographic and symptom characteristics of PTSD (N=961) and control (N=1,124) groups.

Variable	Control	PTSD	Difference	*p* value
N (%)	1,124 (53.9%)	961 (46.1%)		
Female N (%)	487 (43.3%)	519 (54.0%)	χ^2=23.67 (df = 1)	<0.0001*
Male N (%)	637 (56.7%)	442 (46.0%)		
Ages (yrs: mean$\pm$sd)	41.00$\pm$14.41	39.40$\pm$13.08	t=-2.65 (df = 2076)	0.0081*
Age range (yrs)	15-87	16-95		
PTSD Severity	8.64 ± 9.76	49.71$\pm$17.03	t=64.93 (df = 1146.7)	<0.0001*
N of depression High/Low	33/985	283/580	χ^2=289.69 (df = 1)	<0.0001*

Data are reported as mean $\pm$ 1 standard deviation.
df: degrees of freedom
*: significant at $p < 0.05$ level

Male and female subjects between 15 and 95 years old were studied. Compared to controls, participants with PTSD were more likely to be female (*p*<.0001) and were younger in age (*p*=.0081) (**Table 1**). The PTSD group had significantly greater PTSD severity scores (*p*<.0001) and higher comorbid depression than controls (*p*<.0001) (**Table 1**).

3.2 NMF identifies reproducible structural covariance networks

All measures before and after harmonization were reported as mean and standard deviation values for both left and right hemispheres (Table S5). Site-associated differences were removed by ComBat to generate harmonized cortical thickness measurements (Fig. S2, Fig. S3; see also Table S6). NMF analyses delineated SCNs at multiple resolutions ranging from 2 to 40 (in steps

of 2). The 20-SCN solution was selected based on reconstruction error evaluation and split-half reproducibility analysis (Fig. S4). Reconstruction error decreased consistently with increasing resolution and stabilized at 20 networks. Although reproducibility was not uniformly stable, a local peak was clearly present for the 20-SCN. Accordingly, the 20-network solution was used for all subsequent analyses. As in previous work using NMF [35], nearly all structural components were highly symmetric bilaterally (**Fig. 2**).

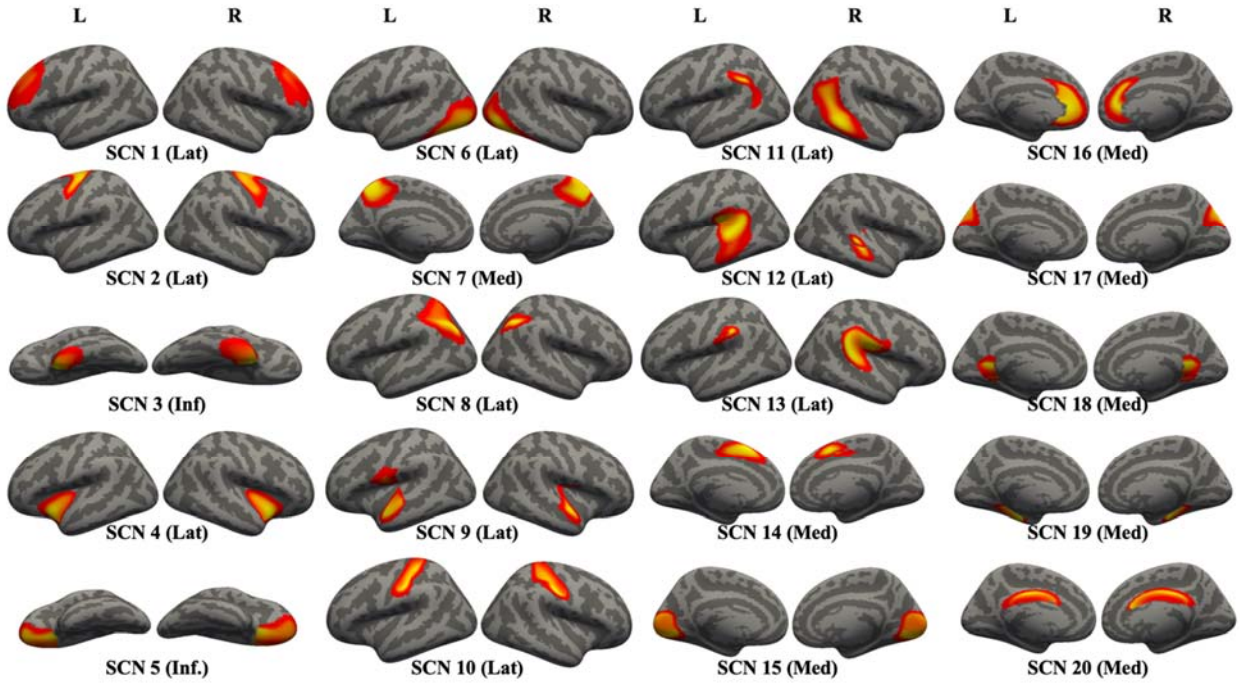

3.3 PTSD is significantly associated with structural differences in multiple networks

Having identified 20 interpretable SCNs using NMF, we next examined associations between mean cortical thickness in each SCN with PTSD diagnosis while controlling for sex, as well as linear and nonlinear age effects (Eq. 1). Univariate analyses revealed that there was a significant association between PTSD diagnosis and cortical thickness measurements in 8 SCNs after FDR correction (**Fig. 3**; see also Table S7), though characterized by small effect sizes. Regions associated with PTSD included the bilateral superior and medial superior frontal cortex (SCN 1 and 14), the motor cortex (SCN 2), the insular cortex (SCN 4), the orbitofrontal cortex (SCN 5), the medial occipital cortex (SCN 15), the anterior and the posterior cingulate cortex (SCN 16

and 18). PTSD diagnosis was associated with lower cortical thickness in each of these networks (Table S7; Table S8). Inclusion of the trauma type as covariate in the regression models consistently produced similar results. The significant associations between the SCNs and PTSD diagnosis remained unchanged (Table S7).

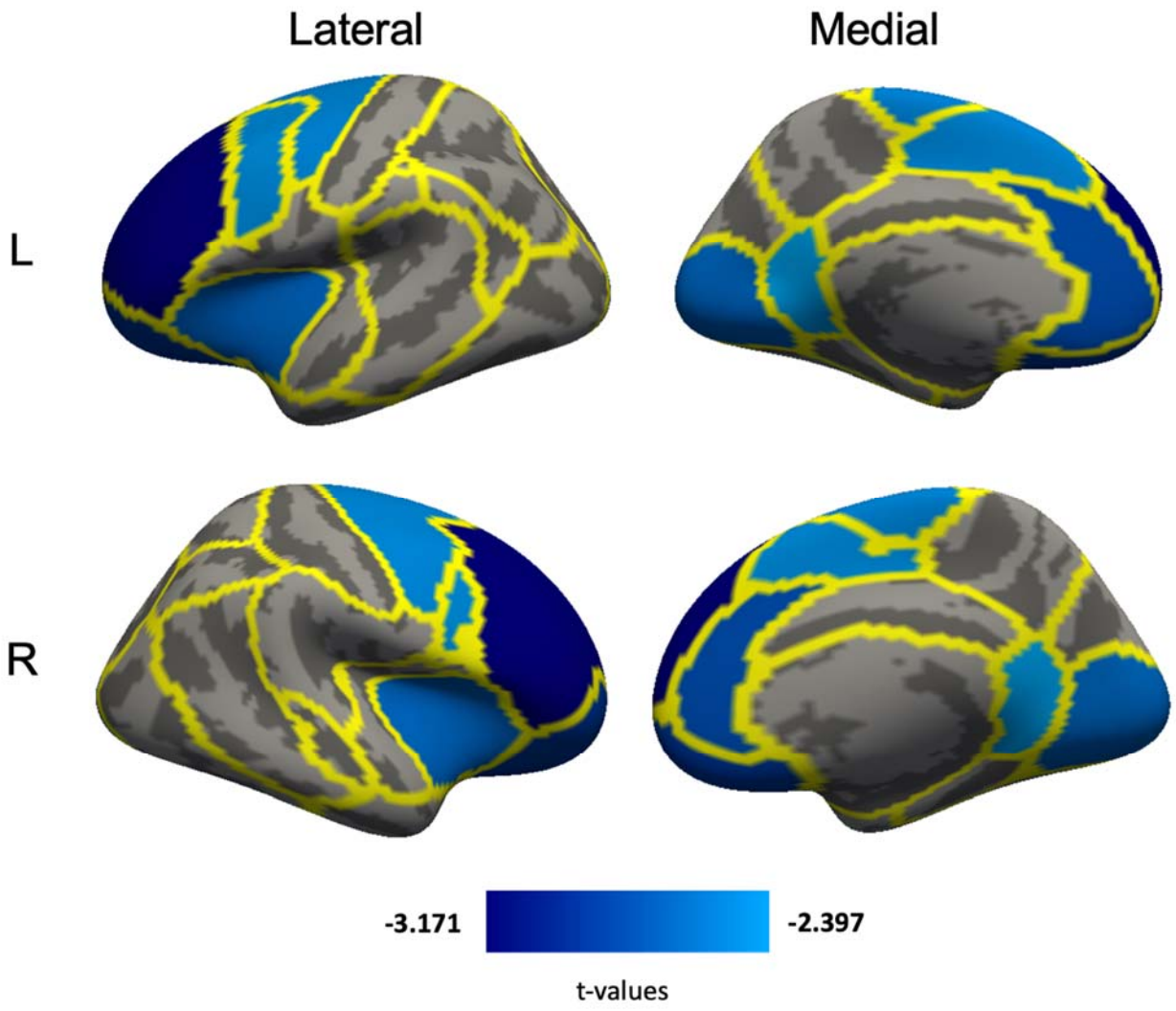

3.4 Association between PTSD diagnosis and SCNs is independent of age and sex

Having established that diminished cortical thickness was associated with PTSD, we next examined whether this effect was moderated by age or sex. Notably, there were no significant interactions of sex and age by PTSD diagnosis in any network (Table S9). Considering age and sex were significantly different between PTSD and control subjects (**Table 1**), we repeated the

NMF analysis in age- and sex-matched subsamples obtained by excluding 4 subsites, including 2 cohorts of young female PTSD patients (Groningen, Mannheim) and 2 cohorts with old male control subjects (Duke-TBIPTSD, Nanjing-Yixing). The rebalanced groups did not show significant age or sex differences (39.66±13.26 years in PTSD vs. 40.10±14.35 years in control, T = 0.69, df = 1886, p = 0.49; 917 female subjects vs. 986 male subjects, χ^2=0.74, df = 1, p = 0.39). Despite the reduced power of the rebalanced groups, 6 of the 8 significant SCNs were still found to be associated with PTSD diagnosis (Table S10) and characterized by small effect sizes. Although the motor cortex (SCN 2) and the posterior cingulate cortex (SCN 18) were not significant in this subsample, they trended toward significance (p_{fdr} = 0.0621 and p_{fdr} = 0.0710, respectively). Again, within all these networks, PTSD diagnosis was associated with lower cortical thickness.

3.5 Regression analysis with PTSS severity yields similar results

We next examined associations between dimensional PTSS severity and cortical thickness across SCNs (Eq. 2). Results revealed that increased PTSS severity was associated with reduced cortical thickness in 8 networks (FDR-corrected; Table S11), though characterized by small effect sizes. Notably, 7 of these 8 networks overlapped with those found to be related to PTSD diagnosis (**Fig. 4**). The posterior cingulate cortex (SCN 18) and the anterior superior temporal gyrus (SCN 9) were the only differences between the categorical and dimensional analyses. The former was FDR-significant in the categorical group analysis, while the latter was FDR-significant in the dimensional analysis. However, the posterior cingulate cortex (SCN 18) trended toward significance in dimensional analysis (p_{fdr} = 0.0621), and the anterior superior temporal gyrus (SCN 9) trended toward significance in the categorical group analysis (p_{fdr} = 0.0547).

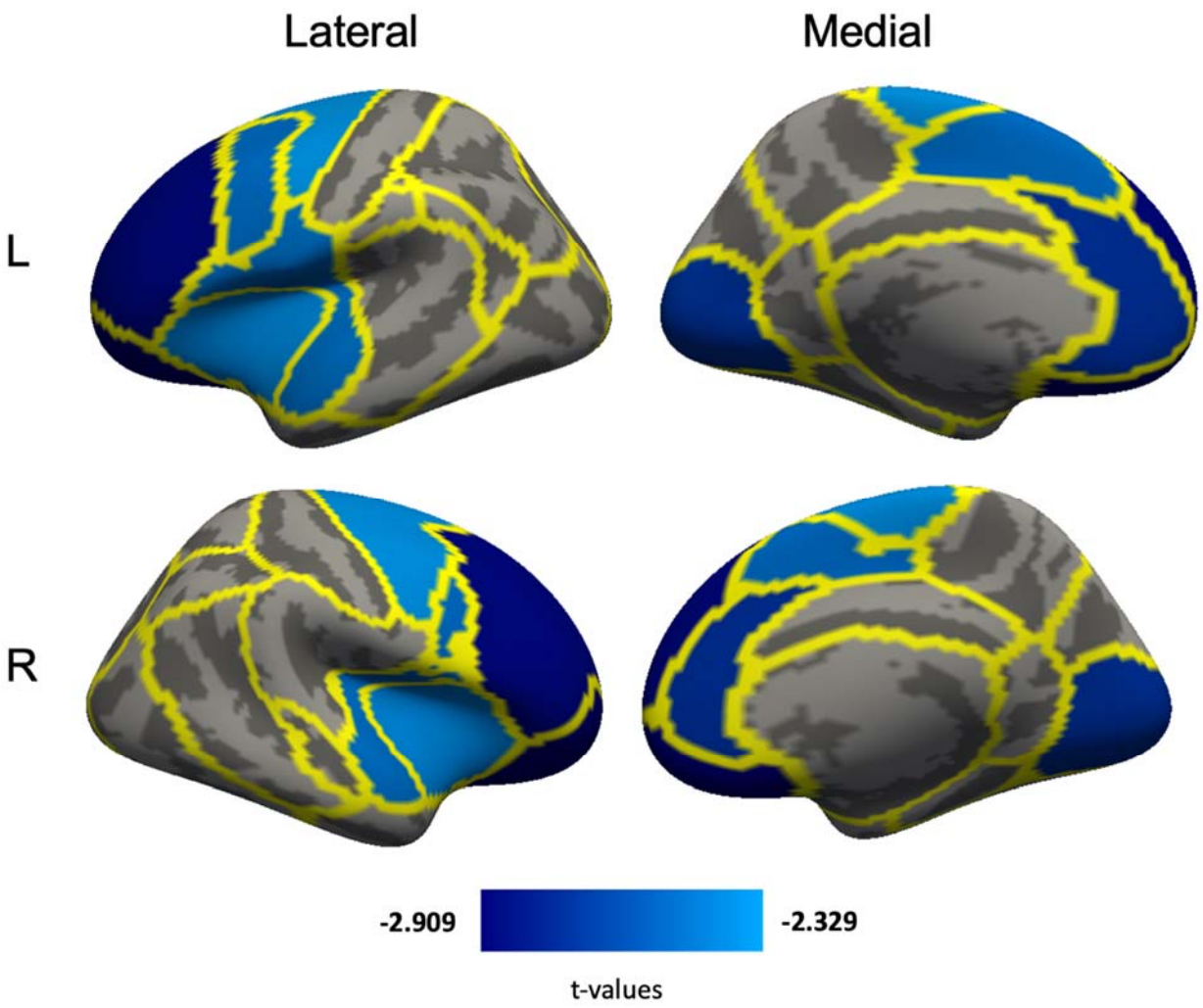

3.6 Significant association with depression level is found in medial occipital cortex

Next, we examined the associations between depression and cortical thickness separately for PTSD participants and all subjects with depression information (Eq. 3). When examining only PTSD participants, no significant effects of depression severity were found in any network (Table S12), suggestive of PTSD-specific cortical thickness associations. When examining the entire sample, cortical thickness in the medial occipital cortex (SCN 15) was found to be significantly associated with depression severity (Fig. S5; see also Table S12), albeit with a small effect size. In this case, subjects with high depression symptoms demonstrated lower cortical thickness in this network compared to those with low depression symptoms. When including categorical PTSD diagnosis and depression in the same regression model (Eq. 4), no significant

associations with SCNs were detected for either depression severity or PTSD diagnosis. This is potentially because of the moderate to strong positive correlation between depression severity and PTSD diagnosis (Pearson correlation coefficient (r) was $r = 0.39$ ($p < 0.001$)), and between depression and PTSS ($r = 0.47$ ($p < 0.001$)). The observed multicollinearity may have effectively lowered the statistical power to detect individual effects of either PTSD or depression. When repeating the primary regression analysis (Eq. 1) in this sub-sample, a statistically significant association between PTSD diagnosis and cortical thickness measurements was detected in the same 8 SCNs as in the full sample (Table S13). The results were characterized by small effect sizes. In summary, the separate analyses for depression and PTSD revealed non-overlapping associations with cortical thickness in distinct SCNs. These findings suggest that the effects observed for PTSD are likely specific to this condition and are not influenced by depression.

3.7 Assessing the association between cortical thickness with childhood trauma severity or alcohol abuse

Lastly, we conducted separate examinations to assess the associations between childhood trauma severity or alcohol use disorder and cortical thickness for all subjects with available corresponding information (Eq. 3). Our analysis, including the full sub-sample, PTSD patients only, and control subjects only, revealed no significant associations between CTQ and SCNs (Table S14). Similarly, we did not identify any significant associations between AUD and SCNs in both the subset of PTSD participants and the full sub-sample (Table S15). Additionally, when we separately assessed the potential confounding effect of childhood trauma or alcohol abuse on PTSD-associated group differences (Eq. 4) in the sub-sample for which CTQ or AUD data was available, no significant associations were detected for CTQ or AUD. Additionally, in these much smaller samples, it was not possible to identify statistically significant effects of PTSD, irrespective of whether we included the confounder in the regression analyses (Eq. 4) or not (Eq. 1).

4. Discussion

In 2,085 participants from 22 international sites, we investigated associations between PTSD and cortical thickness in networks with strong cortical thickness covariance patterns ascertained by NMF. PTSD was associated with decreased cortical thickness in 8 of the 20 distinct SCNs characterized by vertices within the following anatomic structures: bilateral superior and medial superior frontal cortex, motor cortex, insular cortex, orbitofrontal cortex, medial occipital cortex, anterior and posterior cingulate cortex. Including trauma type as covariate in the regression analysis did not change the results. Associations with PTSD symptom severity (rather than diagnosis) were consistent: cortical thickness differences were related to PTSD severity in all networks associated with PTSD diagnosis except for the posterior cingulate cortex. One additional network in the anterior superior temporal gyrus was associated with PTSD symptom severity. The group with moderate/severe comorbid depression symptoms differed from the group with mild comorbid depression symptoms in cortical thickness within the medial occipital cortex. In the sub-samples where CTQ or AUD information was available, we did not identify any significant associations with PTSD, CTQ or AUD, irrespective of whether we ran the regression analysis by separately including only PTSD, only the confounder, or both.

A unique aspect of our study is the two-stage approach with an initial data reduction followed by a hypothesis generation stage. NMF is well suited to tackling inter-individual spatial heterogeneity because it identifies networks without regard to neuroanatomic boundaries. Instead, NMF identifies patterns of thickness covariation that transcend gyral-based ROI boundaries. Prior studies applying NMF to healthy subjects identified patterns of gray matter structural covariance that differed anatomically but aligned closely with functionally defined brain networks [35]. Additionally, SCNs defined by NMF provide a parsimonious summary of high-dimensional data, which may be more interpretable than data reduction with principal component analysis or independent component analysis [34]. Importantly, the concise summary of the data provided by NMF limits multiple comparisons, thus reducing the need for correction that can plague mass-univariate vertex-wise studies. Consequently, we were able to

apply a rigorous FDR correction to all comparisons, instead of relying on cluster-based inference, which may lead to higher rates of type I errors [58].

Another unique aspect of our study is that it represents the largest published cortical thickness study in PTSD to date. The large sample size enhanced our statistical power and sensitivity to detect effects in multiple networks. Despite the small effect sizes observed, extensive prior research has documented that small underpowered studies often yield inflated effect sizes [59,60]. Therefore, our results likely provide a more accurate representation of the true effect size compared to findings from smaller studies. This may explain discrepancies with previous studies reporting increased cortical thickness in smaller samples consisting of 67 patients with PTSD [30], 15 patients with recent onset PTSD [31] and 30 patients who successfully recovered from PTSD [21], respectively. Additional factors might have contributed to the reported differences, including methodological choices. For instance, the use of cluster-based inference employed in [21,30] can lead to significant type I error rates [58].

The present study is comparable in scale and scope to the ENIGMA-PTSD study of regional cortical volume by Wang and colleagues [61] who assessed regional cortical volume (i.e., the product of cortical thickness and cortical surface area for any given region). Despite different analytic approaches, our cortical thickness findings similarly implicate cortical differences within the R-superior frontal gyrus, bilateral orbitofrontal gyrus, insular cortex, L-anterior cingulate gyrus, and L-posterior cingulate gyrus related to PTSD. In addition, we found PTSD to be associated with cortical thickness in the R-anterior cingulate gyrus, R-posterior cingulate gyrus, and the L- superior frontal gyrus, which were not linked to cortical volume. By contrast, Wang et al. (2021) reported cortical volume differences associated with PTSD for several regions, not identified by the present study, including the precuneus, middle temporal gyrus, superior parietal gyrus, and inferior parietal gyrus [61]. As cortical volume captures both cortical thickness and surface area, the latter set of regions may possess stronger associations with regional surface area but may be weakly linked to cortical thickness.

The partially overlapping and partially divergent associations of PTSD to cortical thickness in comparison to cortical volume may relate to the stronger role of genetics in determining cortical surface area than cortical thickness, which is more influenced by environmental factors, effects of PTSD illness, or individual PTSD symptom features [62]. Specifically, cortical volume may better index combined genetic and environmental effects, whereas cortical thickness may capture the deleterious effects of trauma exposure and pathology and cortical surface area may be more influenced by genetic contributors.

In addition to links between cortical structural alterations and PTSD [6,7,13–16], prior evidence links altered cortical structure to brain function in PTSD [63]. Disruption in emotion processing circuits and top-down prefrontal dysregulation of these circuits are linked to PTSD [64]. In this context, the left orbitofrontal gyrus plays an important role in integrating sensory and limbic inputs and in top-down prefrontal inhibitory regulation of emotion and sensory regions [65,66]. Patients with orbitofrontal gyrus lesions demonstrate attention deficits and impaired response inhibition to emotional stimuli [67]. Thus, low left orbitofrontal gyrus thickness/volume may impair inhibitory top-down regulation of emotion and sensory attention. Reduced gray-matter density in the anterior insula has been linked to greater intrusive memories following trauma [68,69], which may explain anterior insula over-responsiveness to negative emotions in PTSD [70]. We found reduced bilateral cortical thickness in the insula, which is consistent with a heightened sensitivity to interoceptive sensations, internal body cues, and a predilection toward threat-biased interpretations, which are common features of PTSD.

Lower cortical thickness in motor cortex and primary visual cortex while unexpected, is nonetheless supported by recent discoveries. In sexual assault survivors with PTSD, reduced gray matter density and functional connectivity within the visual cortex are associated with re-experiencing symptoms and self-blame [71]. These primary sensory regions are activated by intrusive memories that are experienced in PTSD and MDD [72]. Functional MRI studies reveal hyperresponsiveness of the anterior cingulate in PTSD [73], including in monozygotic twins, which represents a familial risk marker for PTSD [74]. Similarly, pre-conscious actions to

mitigate threat or danger in PTSD patients are associated with stronger functional connectivity between motor cortex and periaqueductal gray, which initiates defensive responding [75,76]. The medial occipital cortex, which is well known for primary visual perception, is engaged in feedforward and feed backward signaling of threat or danger [77,78]. A recent demonstration of neuromodulation of the visual cortex reduced the intensity of intrusive trauma memories [79], while treatment directed at modification of attentional bias reduced PTSD symptoms and modulated activity in visual processing pathways. Thus, converging evidence implicates the involvement of primary sensory and motor regions in PTSD [80,81], which may explain reduced cortical thickness in these regions. However, the precise causal mechanisms connecting brain structure to function are unclear, as are the cellular mechanisms of learning-induced grey matter changes. Recent evidence suggests that the remodeling of neuronal processes, which involves presynaptic terminals forming synapses with dendritic spines, as a possible mechanism [82–85].

When we examined associations between cortical thickness and depression symptom severity in PTSD patients, no networks were significantly associated with depression severity. Additionally, when examining associations between cortical thickness and PTSD diagnosis while controlling for depression in the full sub-sample, no networks were significantly associated with PTSD diagnosis. These results have various potential interpretations. First, we found greater depression symptom severity in PTSD patients and greater PTSD symptom severity in depressed subjects, suggesting a positive association between PTSD and depression symptoms. This raises a possibility that variance shared across PTSD and depression effectively lowered the statistical power to detect true PTSD effects [86,87]. Second, symptoms such as negative emotions, cognitive distortions, and avoidance are common to both disorders. Third, it is possible that depression symptoms and PTSD symptom severity are mediated, in part, by shared brain abnormalities. If any or all these explanations are valid, our findings would suggest that lower cortical thickness in some regions could be associated with PTSD. Alternatively, the current results cannot rule out the possibility that thinner cortex in these regions may be associated with depression, but not PTSD.

Several limitations of our study should be considered when interpreting its results. First, while we primarily focused on the 20-network solution as the solution that is both reproducible and fits the data well, the optimal number of networks is likely a function of the input data. Second, data were derived from cohorts that varied in image acquisition, processing, and clinical assessment instruments. We adjusted for data source statistically and had acceptable heterogeneities of cortical regional volumes across cohorts. Third, additional factors could affect cortical thickness (e.g., cohort stratification, medications, duration of illness, trauma type, age at trauma exposure, trauma exposure of control subjects, and other comorbidities including anxiety disorders and substance abuse). However, we were unable to account for the potential effects of these factors on cortical thickness because we lacked reliable and consistent information across sites. To partially address this limitation, we performed additional analyses focusing on trauma type, child trauma severity and alcohol use disorder, which were the most commonly reported additional covariates across sites. When examining the effect of trauma type in the full sample, we did not observe any significant effects of trauma type on SCNs, while the associations between the SCNs and PTSD diagnosis remained unchanged. The effects of CTQ and AUD were separately analyzed in small subsets of the full dataset. We did not observe any significant effects of CTQ or AUD on SCNs. However, we also did not detect any significant effects of PTSD in these small subsets. Thus, the small subsets seem (1) inadequately powered to address the association of PTSD on SCNs, (2) perhaps inadequately powered to reveal associations between CTQ and AUD on the SCNs or possibly (3) there is shared variance between PTSD and CTQ or between PTSD and AUD that is producing a negative result when testing the association between PTSD and SCNs. Ultimately, the small sample size of participants with CTQ and AUD measures is a limitation and their associations with SCNs should be investigated in future analyses. Finally, the cross-sectional data also cannot distinguish the thickness differences that occurred before vs. after trauma exposure. Further studies are needed to examine confounding effects of comorbid disorders, and to identify age-specific PTSD abnormalities.

In summary, NMF identified unbiased patterns of cortical thickness covariation that are marked by low effect sizes and are associated with lower cortical thickness in PTSD. Our findings recapitulate prior reports using ROI and whole brain methods, but also align closely with functionally defined brain networks.

5. Author contributions

Conceptualization: JY, AH, DS, RAM, and AS; methodology: JY, AH, DS, RAM, and AS; formal analysis: JY; resources:, CD, CCH, DJV, JLF, MO, MvZ, SBJK, LN, BS-J, XZ, YN, ARH, SCM, JTB, LAML, MLK, RQ, GML, PŘ, IR, ELD, CRKC, LES, NJ, PMT, DJS, SK, JCI, SS, SdP, LLvdH, LW, YZ, GL, AS, AM, HW, JKD, CS, JIH, IL, AK, MA, NDD, SRS, SGD, TS, DH, DWG, JBN, RJD, CL, TAdeR-C, JUB, BOO, EMG, GM, RAM, AS; writing—original draft: JY, AH, RAM, and AS; writing – review and edition: all authors; visualizations: JY, and AS; supervision: RAM and AS.

6. Funding

The study was supported by ZonMw, the Netherlands organization for Health Research and Development (40-00812-98-10041), and by a grant from the Academic Medical Center Research Council (110614) (Miranda Olff); NIMH K01 MH118428-01 (Suarez-Jimenez); NARSAD 27040 (Xi Zhu); R01 MH105355 (Yuval Neria); RO1 MH111671 and VISN6 MIRECC (Rajendra A. Morey); Grant 01J05415 from the Special Research Fund (BOF) at Ghent University (Sven C. Mueller); K01 MH118467, Julia Kasparian Fund for Neuroscience Research (Lauren A.M. Lebois); R21 MH112956, R01 MH119227, McLean Hospital Trauma Scholars Fund, Barlow Family Fund, Julia Kasaparian Fund for Neuroscience Research (Milissa L. Kaufman); The Natural Science Foundation of Jiangsu Province (No. BK20221554), and the Foundation for the Social Development Project of Jiangsu (No. BE2022705) (Rongfeng Qi); grant no. AZV NV18-7 04-00559 from the Ministry of Health of the Czech Republic, (Pavel Říha); NIH U54 EB020403, R01 MH116147, R01 MH129742 (Christopher R.K. Ching); R01 MH111671, R01 MH117601, R01 AG059874, MJFF 14848 (Neda Jahanshad); Department of Defense award number W81XWH-12-2-0012; ENIGMA was also supported in part by NIH U54 EB020403 from the Big Data to Knowledge (BD2K) program, R56 AG058854, R01 MH116147, R01 MH111671, and P41 EB015922 (Paul M. Thompson); funding from the SAMRC Unit on Risk & Resilience in Mental

Disorders (Dan J. Stein); the South African Research Chairs Initiative in Posttraumatic Stress Disorder through the Department of Science and Technology and the National Research Foundation (Soraya Seedat); the South African Medical Research Council for the “Shared Roots” Flagship Project, Grant no. MRC-RFA-IFSP-01-2013/SHARED ROOTS” through funding received from the South African National Treasury under its Economic Competitiveness and Support Package (Stefan du Plessis); funding by the South African Medical Research Council through its Division of Research Capacity Development under the SAMRC CLINICIAN RESEARCHER (M.D PHD) SCHOLARSHIP PROGRAMME from funding received from the South African National Treasury (Leigh L. van den Heuvel); the National Natural Science Foundation of China (No. U21A20364 and No. 31971020), the Key Project of the National Social Science Foundation of China (No. 20ZDA079), the Key Project of Research Base of Humanities and Social Sciences of Ministry of Education (No.16JJD190006), and the Scientific Foundation of Institute of Psychology, Chinese Academy of Sciences (No. E2CX4115CX) (Li Wang); German Research Foundation grant to J. K. Daniels (numbers DA 1222/4-1 and WA 1539/8-2) (Judith K. Daniels, Anika Sierk, Antje Manthey, Henrik Walter); R01 MH113574 (Israel Liberzon); VA RR&D 1IK2RX000709 (Nicholas D. Davenport); VA RR&D I01RX000622; CDMRP W81XWH-08–2–0038 (Scott R. Sponheim); VA RR&D 1K1RX002325; 1K2RX002922 (Seth G. Disner); German Research Society (Deutsche Forschungsgemeinschaft, DFG; SFB/TRR 58: C06, C07) (Thomas Straube, David Hofmann); Dana Foundation (to Dr. Nitschke); the University of Wisconsin Institute for Clinical and Translational Research (to Dr. Emma Seppala); a National Science Foundation Graduate Research Fellowship (to Dr. Grupe); the National Institute of Mental Health (NIMH) R01-MH043454 and T32-MH018931 (to Dr. Davidson); and a core grant to the Waisman Center from the National Institute of Child Health and Human Development (P30-HD003352); R01 MH106574 (Christine Larson & Terri A. deRoon-Cassini); VA CSR&D 1IK2CX001680; VISN17 Center of Excellence Pilot funding (Evan M. Gordon, Geoffrey May, Steven M. Nelson); VA National Center for PTSD; The Beth K and Stuart Yudofsky Chair in the Neuropsychiatry of Military Post Traumatic Stress Syndrome (Chadi G. Abdallah); R21 MH102634 (Ifat Levy); R01 MH105535 (Ilan Harpaz-Rotem);Department of Veterans Affairs via support for the National Center for PTSD, NIAAA via its support for (P50) Center for the Translational Neuroscience if

Alcohol, and NCATS via its support of (CTSA) Yale Center for Clinical Investigation (John H. Krystal); and R01AG067103 (Aristeidis Sotiras).

The content of this article is the sole responsibility of the authors and does not necessarily reflect the position, policy or official views of the Department of Veterans Affairs, the U.S. Government, the South African Medical Research Council, or any other funding sources listed here.

7. Competing Interests

LAML reports unpaid membership on the Scientific Committee for the International Society for the Study of Trauma and Dissociation (ISSTD), and spousal IP payments from Vanderbilt University for technology licensed to Acadia Pharmaceuticals unrelated to the present work. ISSTD and NIMH were not involved in the analysis or preparation of the manuscript. Dr. Ching received partial research support from Biogen, Inc. (Boston, USA) for research unrelated to the content of this manuscript. Dr. Jahanshad received partial research support from Biogen, Inc. (Boston, USA) for research unrelated to the content of this manuscript. Dr. Thompson received partial research support from Biogen, Inc. (Boston, USA) for research unrelated to the topic of this manuscript. Dr. Davidson is the founder and president of, and serves on the board of directors for, the non-profit organization Healthy Minds Innovations, Inc. Dr. Abdallah has served as a consultant, speaker and/or on advisory boards for Aptinyx, FSV7, Lundbeck, Psilocybin Labs, Genentech, and Janssen; served as editor of Chronic Stress for Sage Publications, Inc; and filed a patent for using mTOR inhibitors to augment the effects of antidepressants (filed on August 20, 2018). Dr. Krystal is a consultant for AbbVie, Inc., Amgen, Astellas Pharma Global Development, Inc., AstraZeneca Pharmaceuticals, Biomedisyn Corporation, Bristol-Myers Squibb, Eli Lilly and Company, Euthymics Bioscience, Inc., Neurovance, Inc., FORUM Pharmaceuticals, Janssen Research & Development, Lundbeck Research USA, Novartis Pharma AG, Otsuka America Pharmaceutical, Inc., Sage Therapeutics, Inc., Sunovion Pharmaceuticals, Inc., and Takeda Industries; is on the Scientific Advisory Board for Lohocla Research Corporation, Mnemosyne Pharmaceuticals, Inc., Naurex, Inc., and Pfizer; is

a stockholder in Biohaven Pharmaceuticals; holds stock options in Mnemosyne Pharmaceuticals, Inc.; holds patents for Dopamine and Noradrenergic Reuptake Inhibitors in Treatment of Schizophrenia, US Patent No. 5,447,948 (issued September 5, 1995), and Glutamate Modulating Agents in the Treatment of Mental Disorders, U.S. Patent No. 8,778,979 (issued July 15, 2014); has filed a patent for Intranasal Administration of Ketamine to Treat Depression. U.S. Application No. 14/197,767 (filed on March 5, 2014); US application or Patent Cooperation Treaty international application No. 14/306,382 (filed on June 17, 2014); and has filed a patent for using mTOR inhibitors to augment the effects of antidepressants (filed on August 20, 2018). Dr. Sotiras holds equity in TheraPanacea and has received personal compensation for serving as a grant reviewer with the BrightFocus Foundation. The remaining authors have nothing to disclose.

References

1. Kilpatrick DG, Resnick HS, Milanak ME, Miller MW, Keyes KM, Friedman MJ. National Estimates of Exposure to Traumatic Events and PTSD Prevalence Using DSM-IV and DSM-5 Criteria. J Trauma Stress. 2013;26:537–547.
2. American Psychiatric Association. Diagnostic and Statistical Manual of Mental Disorders. 5th ed. American Psychiatric Association; 2013.
3. Etkin A, Wager TD. Functional Neuroimaging of Anxiety: A Meta-Analysis of Emotional Processing in PTSD, Social Anxiety Disorder, and Specific Phobia. American Journal of Psychiatry. 2007;164:1476–1488.
4. Karl A, Schaefer M, Malta L, Dorfel D, Rohleder N, Werner A. A meta-analysis of structural brain abnormalities in PTSD. Neurosci Biobehav Rev. 2006;30:1004–1031.
5. O'Doherty DCM, Chitty KM, Saddiqui S, Bennett MR, Lagopoulos J. A systematic review and meta-analysis of magnetic resonance imaging measurement of structural volumes in posttraumatic stress disorder. Psychiatry Res Neuroimaging. 2015;232:1–33.
6. Corbo V, Salat DH, Amick MM, Leritz EC, Milberg WP, McGlinchey RE. Reduced cortical thickness in veterans exposed to early life trauma. Psychiatry Res Neuroimaging. 2014;223:53–60.
7. Geuze E, Westenberg HGM, Heinecke A, de Kloet CS, Goebel R, Vermetten E. Thinner prefrontal cortex in veterans with posttraumatic stress disorder. Neuroimage. 2008;41:675–681.
8. Gold AL, Sheridan MA, Peverill M, Busso DS, Lambert HK, Alves S, et al. Childhood abuse and reduced cortical thickness in brain regions involved in emotional processing. Journal of Child Psychology and Psychiatry. 2016;57:1154–1164.
9. Sadeh N, Spielberg JM, Logue MW, Wolf EJ, Smith AK, Lusk J, et al. SKA2 methylation is associated with decreased prefrontal cortical thickness and greater PTSD severity among trauma-exposed veterans. Mol Psychiatry. 2016;21:357–363.
10. Sullivan DR, Morrison FG, Wolf EJ, Logue MW, Fortier CB, Salat DH, et al. The PPM1F gene moderates the association between PTSD and cortical thickness. J Affect Disord. 2019;259:201–209.
11. Wrocklage KM, Averill LA, Cobb Scott J, Averill CL, Schweinsburg B, Trejo M, et al. Cortical thickness reduction in combat exposed U.S. veterans with and without PTSD. European Neuropsychopharmacology. 2017;27:515–525.
12. Bing X, Ming-guo Q, Ye Z, Jing-na Z, Min L, Han C, et al. Alterations in the cortical thickness and the amplitude of low-frequency fluctuation in patients with post-traumatic stress disorder. Brain Res. 2013;1490:225–232.
13. Crombie KM, Ross MC, Letkiewicz AM, Sartin-Tarm A, Cisler JM. Differential relationships of PTSD symptom clusters with cortical thickness and grey matter volumes among women with PTSD. Sci Rep. 2021;11:1825.
14. Ross MC, Sartin-Tarm AS, Letkiewicz AM, Crombie KM, Cisler JM. Distinct cortical thickness correlates of early life trauma exposure and posttraumatic stress disorder are shared among adolescent and adult females with interpersonal violence exposure. Neuropsychopharmacology. 2021;46:741–749.

15. Lindemer ER, Salat DH, Leritz EC, McGlinchey RE, Milberg WP. Reduced cortical thickness with increased lifetime burden of PTSD in OEF/OIF Veterans and the impact of comorbid TBI. Neuroimage Clin. 2013;2:601–611.
16. Clausen AN, Clarke E, Phillips RD, Haswell C, Morey RA. Combat exposure, posttraumatic stress disorder, and head injuries differentially relate to alterations in cortical thickness in military Veterans. Neuropsychopharmacology. 2020;45:491–498.
17. Woodward SH, Schaer M, Kaloupek DG, Cediel L, Eliez S. Smaller Global and Regional Cortical Volume in Combat-Related Posttraumatic Stress Disorder. Arch Gen Psychiatry. 2009;66:1373.
18. Dickie EW, Brunet A, Akerib V, Armony JL. Anterior cingulate cortical thickness is a stable predictor of recovery from post-traumatic stress disorder. Psychol Med. 2013;43:645–653.
19. Heyn SA, Herringa RJ. Longitudinal cortical markers of persistence and remission of pediatric PTSD. Neuroimage Clin. 2019;24:102028.
20. Jeong H, Lee YJ, Kim N, Jeon S, Jun JY, Yoo SY, et al. Increased medial prefrontal cortical thickness and resilience to traumatic experiences in North Korean refugees. Sci Rep. 2021;11:14910.
21. Lyoo IK, Kim JE, Yoon SJ, Hwang J, Bae S, Kim DJ. The Neurobiological Role of the Dorsolateral Prefrontal Cortex in Recovery From Trauma. Arch Gen Psychiatry. 2011;68:701.
22. Averill LA, Abdallah CG, Pietrzak RH, Averill CL, Southwick SM, Krystal JH, et al. Combat Exposure Severity Is Associated With Reduced Cortical Thickness in Combat Veterans: A Preliminary Report. Chronic Stress. 2017;1.
23. Clouston SAP, Deri Y, Horton M, Tang C, Diminich E, DeLorenzo C, et al. Reduced cortical thickness in World Trade Center responders with cognitive impairment. Alzheimer's & Dementia: Diagnosis, Assessment & Disease Monitoring. 2020;12:e12059.
24. Demers LA, Olson EA, Crowley DJ, Rauch SL, Rosso IM. Dorsal Anterior Cingulate Thickness Is Related to Alexithymia in Childhood Trauma-Related PTSD. PLoS One. 2015;10:e0139807.
25. Knight LK, Naaz F, Stoica T, Depue BE. Lifetime PTSD and geriatric depression symptomatology relate to altered dorsomedial frontal and amygdala morphometry. Psychiatry Res Neuroimaging. 2017;267:59–68.
26. Landré L, Destrieux C, Baudry M, Barantin L, Cottier J-P, Martineau J, et al. Preserved subcortical volumes and cortical thickness in women with sexual abuse-related PTSD. Psychiatry Res Neuroimaging. 2010;183:181–186.
27. Rinne-Albers MA, Boateng CP, van der Werff SJ, Lamers-Winkelman F, Rombouts SA, Vermeiren RR, et al. Preserved cortical thickness, surface area and volume in adolescents with PTSD after childhood sexual abuse. Sci Rep. 2020;10:3266.
28. Rosada C, Bauer M, Golde S, Metz S, Roepke S, Otte C, et al. Childhood trauma and cortical thickness in healthy women, women with post-traumatic stress disorder, and women with borderline personality disorder. Psychoneuroendocrinology. 2023;153:106118.

29. Sun D, Haswell CC, Morey RA, De Bellis MD. Brain structural covariance network centrality in maltreated youth with PTSD and in maltreated youth resilient to PTSD. Dev Psychopathol. 2019;31:557–571.
30. Li S, Huang X, Li L, Du F, Li J, Bi F, et al. Posttraumatic Stress Disorder: Structural Characterization with 3-T MR Imaging. Radiology. 2016;280:537–544.
31. Qi S, Mu Y, Liu K, Zhang J, Huan Y, Tan Q, et al. Cortical inhibition deficits in recent onset PTSD after a single prolonged trauma exposure. Neuroimage Clin. 2013;3:226–233.
32. Li L, Zhang Y, Zhao Y, Li Z, Kemp GJ, Wu M, et al. Cortical thickness abnormalities in patients with post-traumatic stress disorder: A vertex-based meta-analysis. Neurosci Biobehav Rev. 2022;134:104519.
33. Galatzer-Levy IR, Bryant RA. 636,120 Ways to Have Posttraumatic Stress Disorder. Perspectives on Psychological Science. 2013;8:651–662.
34. Sotiras A, Resnick SM, Davatzikos C. Finding imaging patterns of structural covariance via Non-Negative Matrix Factorization. Neuroimage. 2015;108:1–16.
35. Sotiras A, Toledo JB, Gur RE, Gur RC, Satterthwaite TD, Davatzikos C. Patterns of coordinated cortical remodeling during adolescence and their associations with functional specialization and evolutionary expansion. Proceedings of the National Academy of Sciences. 2017;114:3527–3532.
36. Cui Z, Li H, Xia CH, Larsen B, Adebimpe A, Baum GL, et al. Individual Variation in Functional Topography of Association Networks in Youth. Neuron. 2020;106:340-353.e8.
37. Sun D, Adduru VR, Phillips RD, Bouchard HC, Sotiras A, Michael AM, et al. Adolescent alcohol use is linked to disruptions in age-appropriate cortical thinning: an unsupervised machine learning approach. Neuropsychopharmacology. 2023;48:317–326.
38. Kalantar-Hormozi H, Patel R, Dai A, Ziolkowski J, Dong H-M, Holmes A, et al. A cross-sectional and longitudinal study of human brain development: The integration of cortical thickness, surface area, gyrification index, and cortical curvature into a unified analytical framework. Neuroimage. 2023;268:119885.
39. Wang F, Lian C, Wu Z, Zhang H, Li T, Meng Y, et al. Developmental topography of cortical thickness during infancy. Proceedings of the National Academy of Sciences. 2019;116:15855–15860.
40. Pehlivanova M, Wolf DH, Sotiras A, Kaczkurkin A, Moore TM, Ciric R, et al. Diminished Cortical Thickness is Associated with Impulsive Choice in Adolescence. The Journal of Neuroscience. 2018;38:2200–2217.
41. Kaczkurkin AN, Park SS, Sotiras A, Moore TM, Calkins ME, Cieslak M, et al. Evidence for Dissociable Linkage of Dimensions of Psychopathology to Brain Structure in Youths. American Journal of Psychiatry. 2019;176:1000–1009.
42. Jirsaraie RJ, Kaczkurkin AN, Rush S, Piiwia K, Adebimpe A, Bassett DS, et al. Accelerated cortical thinning within structural brain networks is associated with irritability in youth. Neuropsychopharmacology. 2019;44:2254–2262.
43. Luking KR, Jirsaraie RJ, Tillman R, Luby JL, Barch DM, Sotiras A. Timing and Type of Early Psychopathology Symptoms Predict Longitudinal Change in Cortical Thickness From Middle Childhood Into Early Adolescence. Biol Psychiatry Cogn Neurosci Neuroimaging. 2022;7:397–405.

44. Neufeld NH, Kaczkurkin AN, Sotiras A, Mulsant BH, Dickie EW, Flint AJ, et al. Structural brain networks in remitted psychotic depression. Neuropsychopharmacology. 2020;45:1223–1231.
45. Yang W, Jin S, Duan W, Yu H, Ping L, Shen Z, et al. The effects of childhood maltreatment on cortical thickness and gray matter volume: a coordinate-based meta-analysis. Psychol Med. 2023;53:1681–1699.
46. Li Q, Zhao Y, Chen Z, Long J, Dai J, Huang X, et al. Meta-analysis of cortical thickness abnormalities in medication-free patients with major depressive disorder. Neuropsychopharmacology. 2020;45:703–712.
47. Suh JS, Schneider MA, Minuzzi L, MacQueen GM, Strother SC, Kennedy SH, et al. Cortical thickness in major depressive disorder: A systematic review and meta-analysis. Prog Neuropsychopharmacol Biol Psychiatry. 2019;88:287–302.
48. Debell F, Fear NT, Head M, Batt-Rawden S, Greenberg N, Wessely S, et al. A systematic review of the comorbidity between PTSD and alcohol misuse. Soc Psychiatry Psychiatr Epidemiol. 2014;49:1401–1425.
49. Rytwinski NK, Scur MD, Feeny NC, Youngstrom EA. The Co-Occurrence of Major Depressive Disorder Among Individuals With Posttraumatic Stress Disorder: A Meta-Analysis. J Trauma Stress. 2013;26:299–309.
50. Fischl B. FreeSurfer. Neuroimage. 2012;62:774–781.
51. Fortin JP, Cullen N, Sheline YI, Taylor WD, Aselcioglu I, Cook PA, et al. Harmonization of cortical thickness measurements across scanners and sites. Neuroimage. 2018;167:104–120.
52. Logue MW, van Rooij SJH, Dennis EL, Davis SL, Hayes JP, Stevens JS, et al. Smaller Hippocampal Volume in Posttraumatic Stress Disorder: A Multisite ENIGMA-PGC Study: Subcortical Volumetry Results From Posttraumatic Stress Disorder Consortia. Biol Psychiatry. 2018;83:244–253.
53. Fortin JP, Parker D, Tunç B, Watanabe T, Elliott MA, Ruparel K, et al. Harmonization of multi-site diffusion tensor imaging data. Neuroimage. 2017;161:149–170.
54. Radua J, Vieta E, Shinohara R, Kochunov P, Quidé Y, Green MJ, et al. Increased power by harmonizing structural MRI site differences with the ComBat batch adjustment method in ENIGMA. Neuroimage. 2020;218:116956.
55. Bernstein DP, Fink L, Handelsman L, Foote J, Lovejoy M, Wenzel K, et al. Initial reliability and validity of a new retrospective measure of child abuse and neglect. American Journal of Psychiatry. 1994;151:1132–1136.
56. Benjamini Y, Hochberg Y. Controlling the False Discovery Rate: A Practical and Powerful Approach to Multiple Testing. Journal of the Royal Statistical Society: Series B (Methodological). 1995;57:289–300.
57. https://www.rdocumentation.org/packages/stats/versions/3.6.2/topics/p.adjust.
58. Eklund A, Nichols TE, Knutsson H. Cluster failure: Why fMRI inferences for spatial extent have inflated false-positive rates. Proceedings of the National Academy of Sciences. 2016;113:7900–7905.
59. Button KS, Ioannidis JPA, Mokrysz C, Nosek BA, Flint J, Robinson ESJ, et al. Power failure: why small sample size undermines the reliability of neuroscience. Nat Rev Neurosci. 2013;14:365–376.

60. Marek S, Tervo-Clemmens B, Calabro FJ, Montez DF, Kay BP, Hatoum AS, et al. Reproducible brain-wide association studies require thousands of individuals. Nature. 2022;603:654–660.
61. Wang X, Xie H, Chen T, Cotton AS, Salminen LE, Logue MW, et al. Cortical volume abnormalities in posttraumatic stress disorder: an ENIGMA-psychiatric genomics consortium PTSD workgroup mega-analysis. Mol Psychiatry. 2020. 2020. https://doi.org/10.1038/s41380-020-00967-1.
62. Grasby KL, Jahanshad N, Painter JN, Colodro-Conde L, Bralten J, Hibar DP, et al. The genetic architecture of the human cerebral cortex. Science (1979). 2020;367.
63. Fonzo GA, Flagan TM, Sullivan S, Allard CB, Grimes EM, Simmons AN, et al. Neural functional and structural correlates of childhood maltreatment in women with intimate-partner violence-related posttraumatic stress disorder. Psychiatry Res Neuroimaging. 2013;211:93–103.
64. Liberzon I, Abelson JL. Context Processing and the Neurobiology of Post-Traumatic Stress Disorder. Neuron. 2016;92:14–30.
65. Aupperle RL, Allard CB, Grimes EM, Simmons AN, Flagan T, Behrooznia M, et al. Dorsolateral prefrontal cortex activation during emotional anticipation and neuropsychological performance in posttraumatic stress disorder. Arch Gen Psychiatry. 2012;69:360–371.
66. Hooker CI, Knight RT. The role of lateral orbitofrontal cortex in the inhibitory control of emotion. The Orbitofrontal Cortex, Oxford University PressOxford; 2006. p. 307–324.
67. Rule RR, Shimamura AP, Knight RT. Orbitofrontal cortex and dynamic filtering of emotional stimuli. Cogn Affect Behav Neurosci. 2002;2:264–270.
68. Herringa R, Phillips M, Almeida J, Insana S, Germain A. Post-traumatic stress symptoms correlate with smaller subgenual cingulate, caudate, and insula volumes in unmedicated combat veterans. Psychiatry Res Neuroimaging. 2012;203:139–145.
69. Kasai K, Yamasue H, Gilbertson MW, Shenton ME, Rauch SL, Pitman RK. Evidence for Acquired Pregenual Anterior Cingulate Gray Matter Loss from a Twin Study of Combat-Related Posttraumatic Stress Disorder. Biol Psychiatry. 2008;63:550–556.
70. Pitman RK, Rasmusson AM, Koenen KC, Shin LM, Orr SP, Gilbertson MW, et al. Biological studies of post-traumatic stress disorder. Nat Rev Neurosci. 2012;13:769–787.
71. Berman Z, Assaf Y, Tarrasch R, Joel D. Assault-related self-blame and its association with PTSD in sexually assaulted women: an MRI inquiry. Soc Cogn Affect Neurosci. 2018;13:775–784.
72. Brewin CR, Gregory JD, Lipton M, Burgess N. Intrusive images in psychological disorders: Characteristics, neural mechanisms, and treatment implications. Psychol Rev. 2010;117:210–232.
73. Kim MJ, Chey J, Chung A, Bae S, Khang H, Ham B, et al. Diminished rostral anterior cingulate activity in response to threat-related events in posttraumatic stress disorder. J Psychiatr Res. 2008;42:268–277.
74. Shin LM, Bush G, Milad MR, Lasko NB, Brohawn KH, Hughes KC, et al. Exaggerated Activation of Dorsal Anterior Cingulate Cortex During Cognitive Interference: A Monozygotic Twin Study of Posttraumatic Stress Disorder. American Journal of Psychiatry. 2011;168:979–985.

75. Harricharan S, Rabellino D, Frewen PA, Densmore M, Théberge J, McKinnon MC, et al. <scp>fMRI</scp> functional connectivity of the periaqueductal gray in <scp>PTSD</scp> and its dissociative subtype. Brain Behav. 2016;6:e00579.
76. Webb EK, Huggins AA, Belleau EL, Taubitz LE, Hanson JL, DeRoon-Cassini TA, et al. Acute Posttrauma Resting-State Functional Connectivity of Periaqueductal Gray Prospectively Predicts Posttraumatic Stress Disorder Symptoms. Biol Psychiatry Cogn Neurosci Neuroimaging. 2020;5:891–900.
77. Morey RA, Lancaster SC, Haswell CC. Trauma Re-experiencing Symptoms Modulate Topology of Intrinsic Functional Networks. Biol Psychiatry. 2015;78:156–158.
78. Todd RM, MacDonald MJ, Sedge P, Robertson A, Jetly R, Taylor MJ, et al. Soldiers With Posttraumatic Stress Disorder See a World Full of Threat: Magnetoencephalography Reveals Enhanced Tuning to Combat-Related Cues. Biol Psychiatry. 2015;78:821–829.
79. Herz N, Bar-Haim Y, Tavor I, Tik N, Sharon H, Holmes EA, et al. Neuromodulation of Visual Cortex Reduces the Intensity of Intrusive Memories. Cerebral Cortex. 2022;32:408–417.
80. Badura-Brack A, McDermott TJ, Heinrichs-Graham E, Ryan TJ, Khanna MM, Pine DS, et al. Veterans with PTSD demonstrate amygdala hyperactivity while viewing threatening faces: A MEG study. Biol Psychol. 2018;132:228–232.
81. Lazarov A, Bar-Haim Y. Emerging Domain-Based Treatments for Pediatric Anxiety Disorders. Biol Psychiatry. 2021;89:716–725.
82. Lerch JP, Yiu AP, Martinez-Canabal A, Pekar T, Bohbot VD, Frankland PW, et al. Maze training in mice induces MRI-detectable brain shape changes specific to the type of learning. Neuroimage. 2011;54:2086–2095.
83. Taubert M, Lohmann G, Margulies DS, Villringer A, Ragert P. Long-term effects of motor training on resting-state networks and underlying brain structure. Neuroimage. 2011;57:1492–1498.
84. Weisberg SM, Ekstrom AD. Hippocampal volume and navigational ability: The map(ping) is not to scale. Neurosci Biobehav Rev. 2021;126:102–112.
85. Miller GA, Chapman JP. Misunderstanding analysis of covariance. J Abnorm Psychol. 2001;110:40–48.
86. Elhai JD, de Francisco Carvalho L, Miguel FK, Palmieri PA, Primi R, Frueh BC. Testing whether posttraumatic stress disorder and major depressive disorder are similar or unique constructs. Journal of anxiety disorders. 2011 Apr 1;25(3):404-10.
87. Stander VA, Thomsen CJ, Highfill-McRoy RM. Etiology of depression comorbidity in combat-related PTSD: a review of the literature. Clinical psychology review. 2014 Mar 1;34(2): 87-98.

Figure legends

Figure 1 Workflow A) We created cortical thickness maps for each subject from T1 sMRI data preprocessed using the FreeSurfer software. Cortical thickness measurements for all subjects were arrayed column-wise to form a cortical thickness matrix. B) Cortical thickness data was harmonized using Combat to remove variation introduced by site-specific acquisition protocols and MRI scanners. C) We applied non-negative matrix factorization (NMF) on the ComBat-harmonized cortical thickness matrix X to identify structural covariance networks. NMF decomposed this input matrix X into a component matrix W and a coefficient matrix H. The component matrix W represents estimated networks (columns) and their loadings on each vertex (rows); the example map shows loadings from one network and corresponds to a column in the W matrix. The weight matrix H provides the subject-specific weights (columns) for each network (rows); the histogram shows CT scores in a single network and corresponds to a row in the H matrix. D) Split-half reproducibility analysis and reconstruction quality evaluation were performed to select the optimal model. E) Once the optimal solution was selected, regression analyses were performed to examine associations between each network and PTSD diagnosis, PTSD severity scores and depression symptom severity, respectively.

Figure 2. Structural covariance networks delineated by NMF are shown for the 20-network solution. The spatial distribution of each network is indicated by loadings at each vertex in arbitrary units (warmer colors represent higher loadings). High symmetry can be found between left (L) and right (R) hemisphere. The anatomic coverage of each structural covariance network was as follows: 1) superior frontal cortex (Lateral); 2) motor cortex (Lateral); 3) temporal pole (Inferior); 4) insular cortex (Lateral); 5) orbitofrontal cortex (Inferior); 6) lateral occipital cortex (Lateral); 7) precuneus (Medial); 8) left superior parietal cortex (Lateral); 9) anterior superior temporal gyrus (Lateral); 10) primary somatosensory cortex (Lateral); 11) right middle temporal gyrus (Lateral); 12) posterior middle temporal gyrus (Lateral); 13) temporoparietal junction (Lateral); 14) medial superior frontal cortex (Medial); 15) medial occipital cortex (Medial); 16) anterior cingulate cortex (Medial); 17) cuneus (Medial); 18) posterior cingulate cortex (Medial); 19) fusiform gyrus (Medial); and 20) middle cingulate gyrus (Medial). Since the networks were defined using a data-driven process, the anatomic naming is intended to be a rough approximation for the location, not a precise description.

Figure 3. Regression analysis results revealed that PTSD diagnosis was associated with thinner cortex in multiple SCNs. The composite network visualization was obtained by assigning each vertex to the network that has the highest loading for that vertex (from the W matrix), across all 20 networks. This association was maximal in SCNs 1 and 5, which included superior frontal cortex (SCN 1) and orbitofrontal cortex (SCN 5). Significant associations were also present in SCNs that included the motor cortex (SCN 2), insular cortex (SCN 4), medial superior frontal cortex (SCN 14), medial occipital cortex (SCN 15), anterior cingulate cortex (SCN 16), and posterior cingulate cortex (SCN 18). Both significant and non-significant SCNs are annotated with boundaries. Lateral and medial views of these significant SCNs are shown for left and right hemisphere, respectively.

Figure 4. Regression analysis results revealed that PTSS severity score was associated with thinner cortex in multiple SCNs. This association was maximal in SCNs 1 and 5, which included superior frontal cortex (SCN 1) and orbitofrontal cortex (SCN 5). Significant associations were also present in SCNs that included the motor cortex (SCN 2), insular cortex (SCN 4), anterior superior temporal gyrus (SCN 9), medial superior frontal cortex (SCN 14), medial occipital cortex (SCN 15), and anterior cingulate cortex (SCN 16). Both significant and non-significant SCNs are annotated with boundaries. Lateral and medial views of these significant SCNs are shown for left and right hemisphere, respectively.

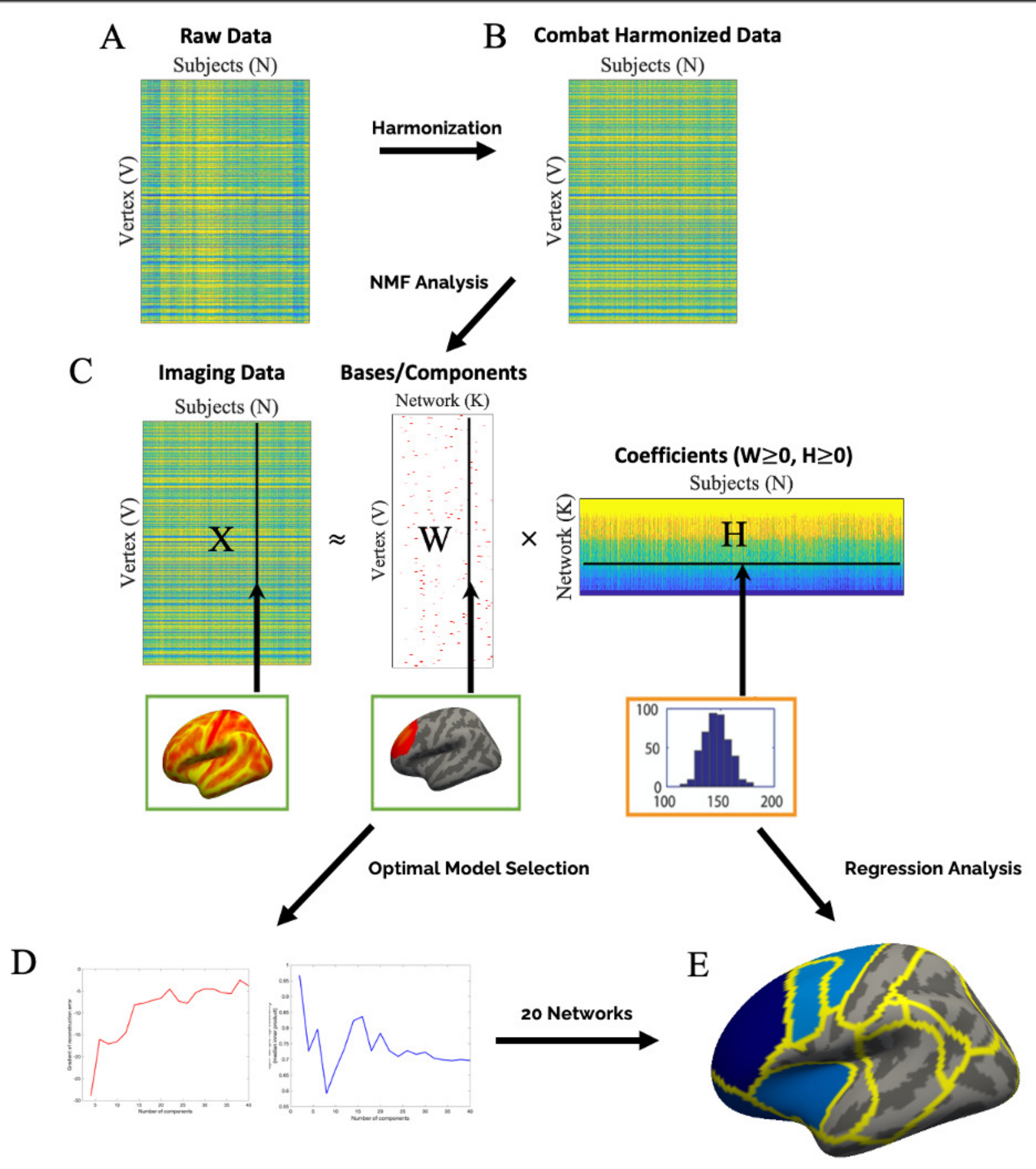
A
Raw Data
Subjects (N)
Vertex (V)
B
Combat Harmonized Data
Subjects (N)
Vertex (V)
Harmonization
NMF Analysis
C
Imaging Data
Subjects (N)
Vertex (V)
X
≈
Bases/Components
Network (K)
Vertex (V)
W
×
Coefficients (W≥0, H≥0)
Subjects (N)
Network (K)
H
100
50
0
100
150
200
Optimal Model Selection
Regression Analysis
D
Number of components
Number of components
20 Networks
E

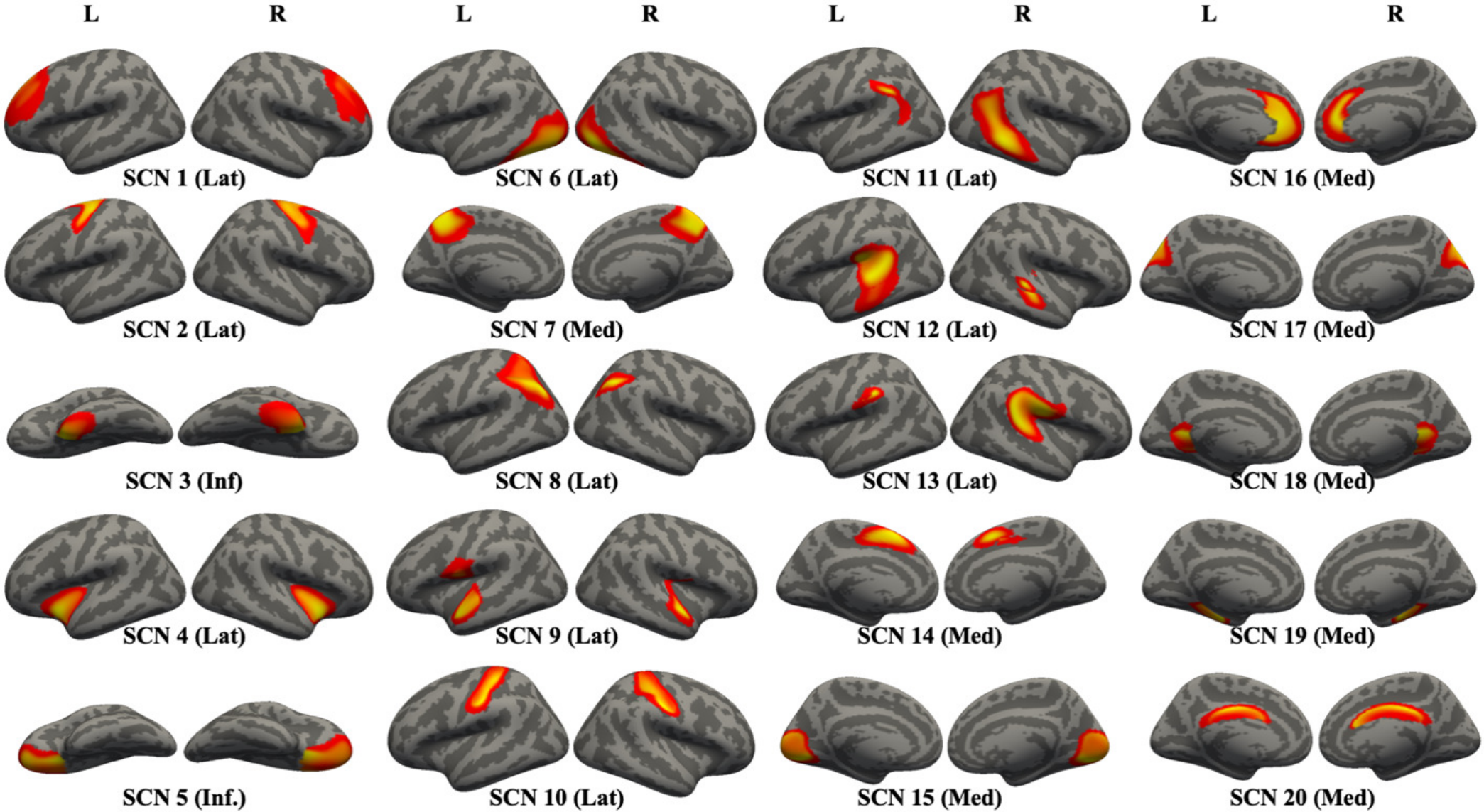
L
R
L
R
L
R
L
R
SCN 1 (Lat)
SCN 6 (Lat)
SCN 11 (Lat)
SCN 16 (Med)
SCN 2 (Lat)
SCN 7 (Med)
SCN 12 (Lat)
SCN 17 (Med)
SCN 3 (Inf)
SCN 8 (Lat)
SCN 13 (Lat)
SCN 18 (Med)
SCN 4 (Lat)
SCN 9 (Lat)
SCN 14 (Med)
SCN 19 (Med)
SCN 5 (Inf.)
SCN 10 (Lat)
SCN 15 (Med)
SCN 20 (Med)

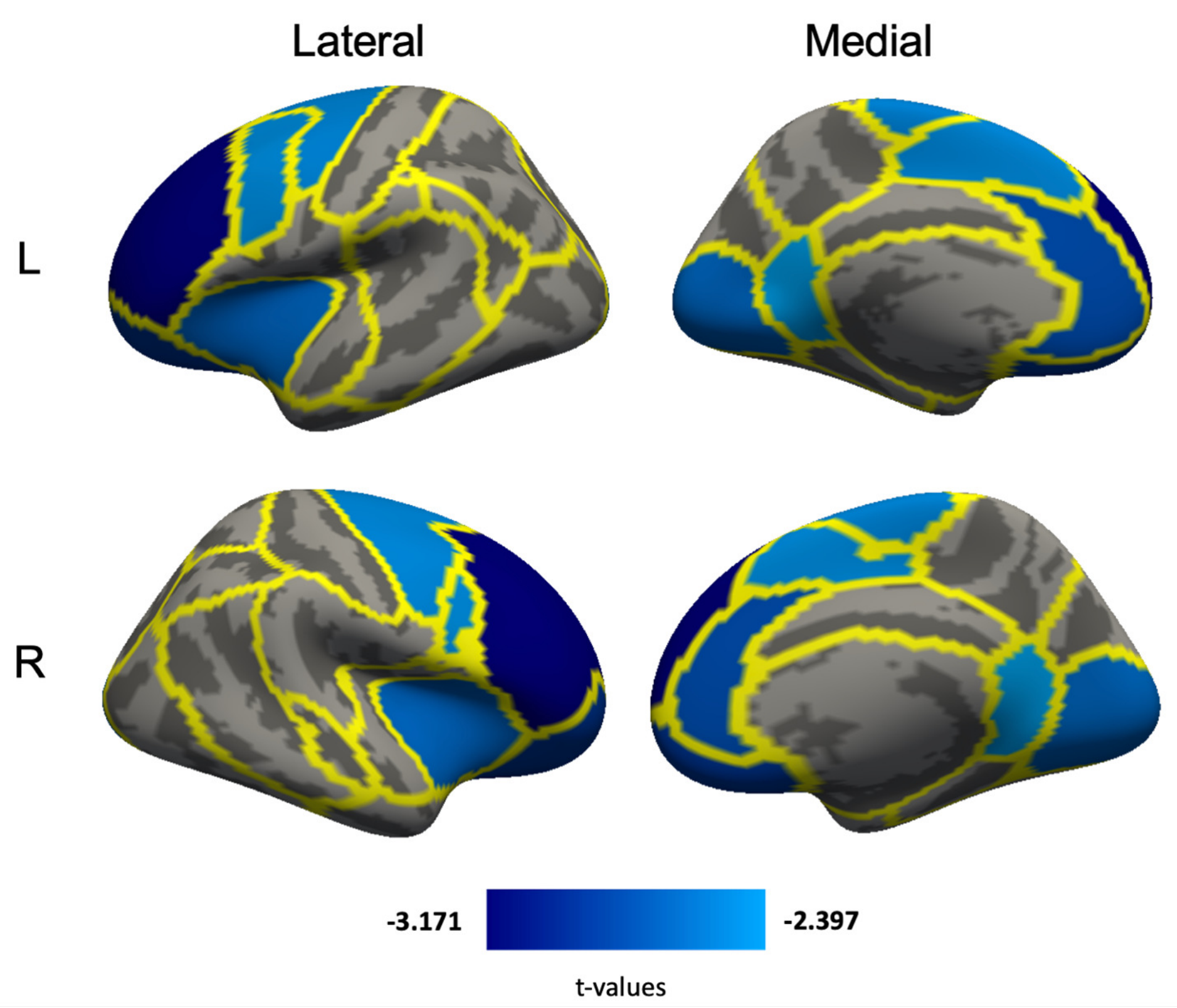
Lateral
Medial
L
R
-3.171
-2.397
t-values

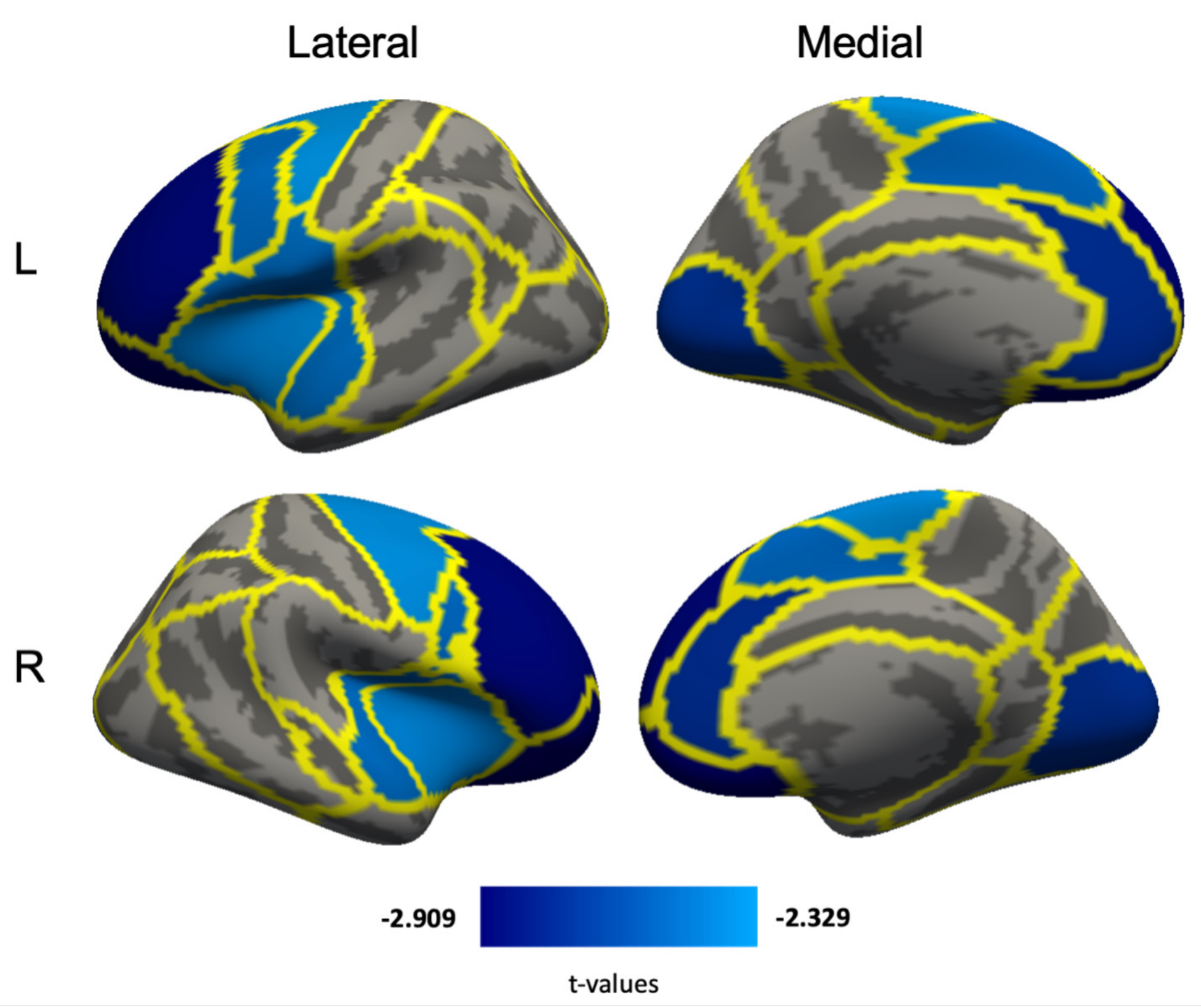
Lateral
Medial
L
R
-2.909
-2.329
t-values

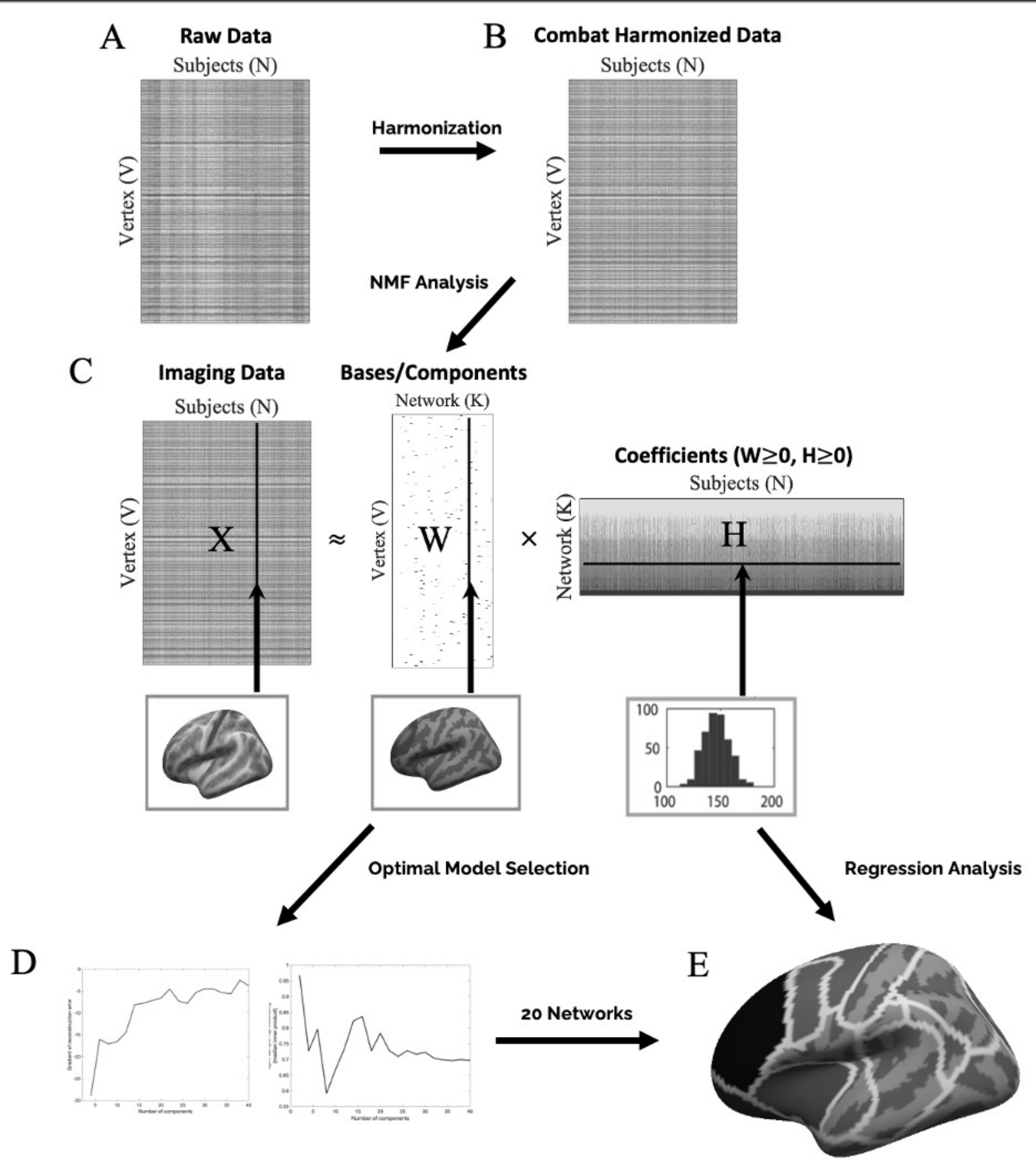
A
Raw Data
Subjects (N)
Vertex (V)
B
Combat Harmonized Data
Subjects (N)
Vertex (V)
Harmonization
NMF Analysis
C
Imaging Data
Subjects (N)
Vertex (V)
X
≈
Bases/Components
Network (K)
Vertex (V)
W
×
Coefficients (W≥0, H≥0)
Subjects (N)
Network (K)
H
100
50
0
100
150
200
Optimal Model Selection
Regression Analysis
D
Number of components
Number of components
20 Networks
E

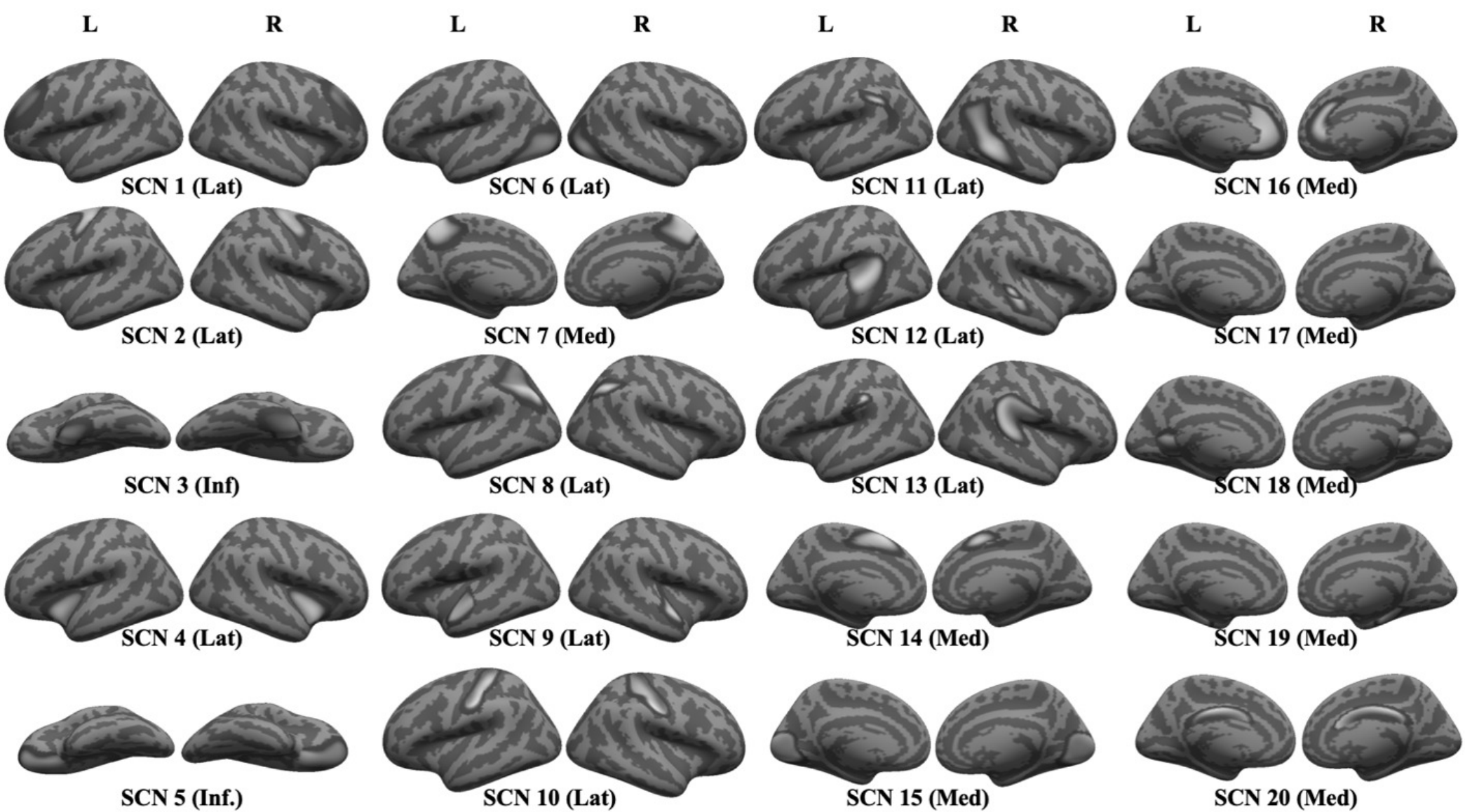
L
R
L
R
L
R
L
R
SCN 1 (Lat)
SCN 6 (Lat)
SCN 11 (Lat)
SCN 16 (Med)
SCN 2 (Lat)
SCN 7 (Med)
SCN 12 (Lat)
SCN 17 (Med)
SCN 3 (Inf)
SCN 8 (Lat)
SCN 13 (Lat)
SCN 18 (Med)
SCN 4 (Lat)
SCN 9 (Lat)
SCN 14 (Med)
SCN 19 (Med)
SCN 5 (Inf.)
SCN 10 (Lat)
SCN 15 (Med)
SCN 20 (Med)

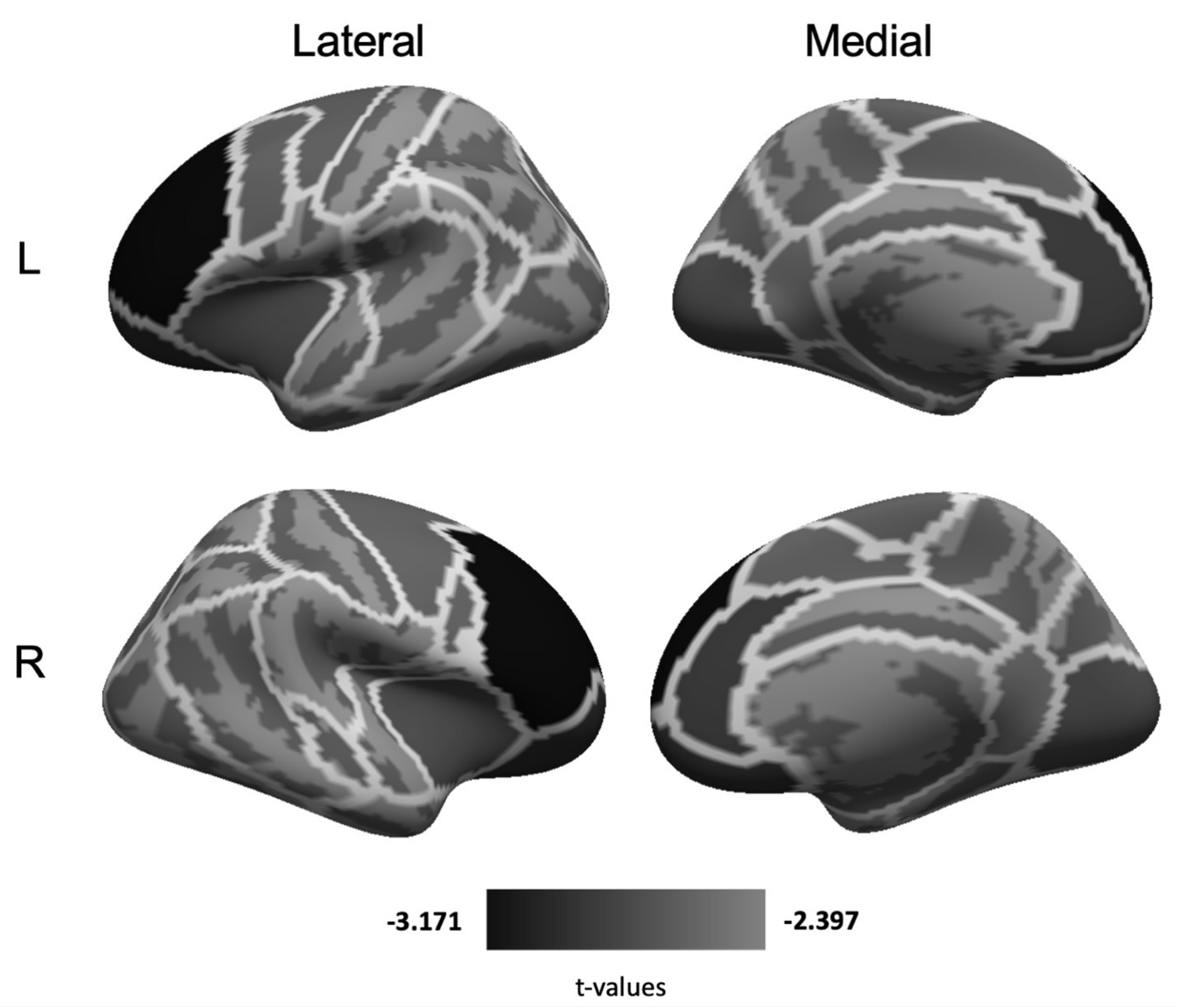
Lateral
Medial
L
R
-3.171
-2.397
t-values

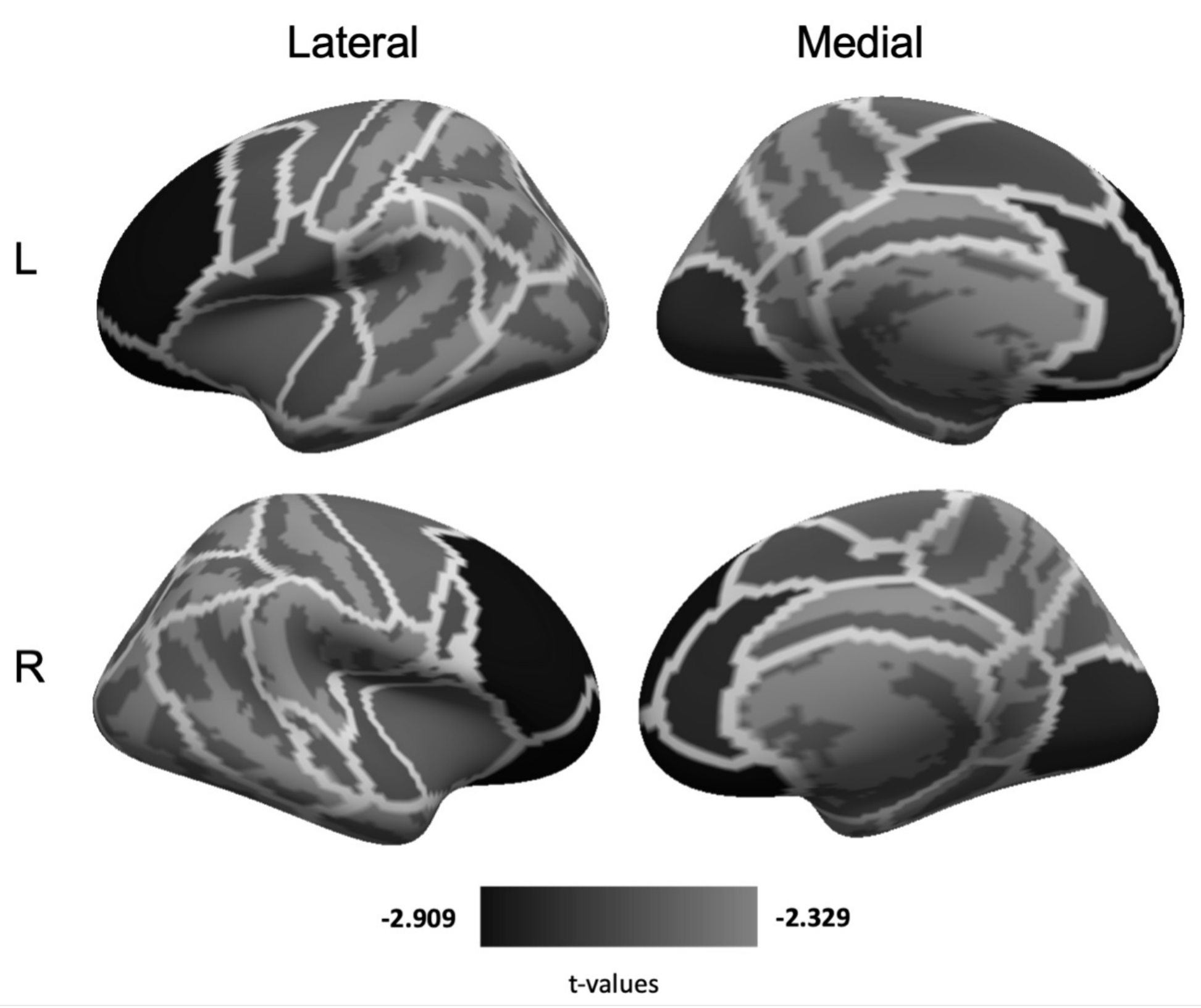
Lateral
Medial
L
R
-2.909
-2.329
t-values